• U C •

FCTUC FACULDADE DE CIÊNCIAS E TECNOLOGIA
UNIVERSIDADE DE COIMBRA

DEPARTAMENTO DE ENGENHARIA MECÂNICA

Analysis of the influence of process parameters in the deep drawing of a cylindrical cup

Submitted in Partial Fulfilment of the Requirements for the Degree of Master of Science in Mechanical Engineering in Production Systems Speciality

Author

Vasco Manuel Neto Simões

Advisors

Luís Filipe Martins Menezes

Hervé Laurent

Jury

President	**Marta Cristina Cardoso de Oliveira** **Professora Auxiliar da Universidade de Coimbra**
Vowels	**Luís Filipe Martins Menezes** **Professor Catedrático da Universidade de Coimbra**
	Hervé Laurent **Professor Auxiliar com Agregação da Universidade de Bretagne-Sud**
	Albano Augusto Cavaleiro Rodrigues de Carvalho **Professor Catedrático da Universidade de Coimbra**
	Cristina Maria Gonçalves dos Santos Louro **Professora Auxiliar da Universidade de Coimbra**

Université de Bretagne-Sud

UBS Université de Bretagne-Sud

LIMATB Laboratoire d'Ingénierie des MATériaux de Bretagne

Coimbra, July 2012

Men love to wonder, and that is the seed of science.

Ralph Waldo Emerson

To my Parents and Sister.

Acknowledgements

The work presented was possible due to the collaboration and support of some people, for which I want to show my gratitude .

My supervisors, Prof. Dr. Luís Menezes and Prof. Dr. Hervé Laurent, for the many discussions and suggestions regarding the research.

Prof. Dr. Marta Oliveira and Jeremy Cöer, for your availability and great help in carrying out my work.

LIMATB and CEMUC teams, for all the technical support, help and liveliness which encouraged me to do more and better of my work.

My parents, for all the help and dedication. Without your encouragement I would never have come so far.

My sister, for all the protection of eldest sister.

Leonor, for all the great moments that we spent together, for the help and friendship.

My friends, for all the coffee breaks; moments of study; academic life; and for your patience, due to your friendship the lasts years were amazing.

Without your contribution, this work would not be possible.

For all of you, my thanks.

Resumo

Actualmente, os processos de estampagem de chapas metálica são usados para produzir uma grande parte dos componentes metálicos que utilizamos no nosso dia-a-dia. O bom acabamento superficial dos componentes, associado ao reduzido custo por peça devido à elevada cadência de produção, são alguns dos factores que contribuem para a selecção preferencial do processo de estampagem na indústria automóvel. Actualmente, a simulação numérica tem um papel fundamental no estudo do processo e na previsão de alguns defeitos. O retorno elástico é um dos defeitos com maior impacto no sucesso de uma operação de estampagem. Assim, têm sido desenvolvidos vários estudos com o objectivo de melhor a previsão deste fenómeno. Um dos testes propostos para estudar o fenómeno de retorno elástico é o ensaio de Demeri, que consiste na estampagem de uma taça cilíndrica, seguido do corte de um anel na parede vertical e no corte transversal desse anel. A abertura do anel é uma medida directa do retorno elástico, que pela sua simplicidade permite uma fácil comparação entre os resultados numéricos e experimentais.

O estudo descrito neste trabalho resulta de uma parceria entre o CEMUC e o LIMATB, com o objectivo de analisar o processo de estampagem de uma taça cilíndrica, correspondente à primeira etapa do ensaio de Demeri. O material seleccionado é uma liga de alumínio AA5754-O, uma vez que se procura aumentar a sua utilização na indústria automóvel, devido às suas boas propriedades mecânicas. No entanto, caracterizam-se também por apresentarem elevados valores de retorno elástico. Neste trabalho analisa-se o efeito de parâmetros como: (i) a variação das dimensões da matriz; (ii) a influência das condições de contacto com atrito; e (iii) a influência das pressões de contacto, na produção de taças cilíndricas com estiramento da parede vertical. A análise destes parâmetros é realizada com o auxílio da simulação numérica e de ensaios experimentais.

A simulação numérica do processo foi realizada com o programa DD3IMP, desenvolvido no CEMUC, e a análise experimental foi efectuada no LIMATB. A análise das forças associadas ao processo e a distribuição da espessura da taça permitiu uma melhor compreensão acerca da influência dos parâmetros em estudo. A principal conclusão deste trabalho é que a ferramenta com maior impacto no processo de conformação é a

matriz, uma vez que o seu diâmetro interno dita a sua folga em relação ao punção e é a ferramenta para a qual ocorrem as maiores pressões de contacto com a chapa. Estes resultados obtidos da análise numérica são corroborados pela análise experimental.

Palavras-chave Estampagem, Simulação numérica, Atrito, Lubricação, Estiramento da parede vertical, Retorno elástico, Dimenções da matriz.

Abstract

Nowadays, sheet metal forming process allow high rates of metal components used in our daily life. Components with smooth surfaces associated to the low cost per part, due to the high rate of production, are the main factors which make this process the first choice for the automotive industry. Currently, numerical simulation has a key role in the study of the forming processes and defects prediction. The springback is one of the defects with the greatest influence on the success of stamping operations. Thus, several studies have been developed in order to better predict this phenomenon. The benchmark test proposed for studying the springback phenomenon is the Demeri test which consists in cutting a ring specimen from a full drawn cup and then splitting the ring longitudinally along a radial plane. The ring opening gives a direct measure of the springback phenomenon which, due to its simplicity, allows the direct comparison between the numerical and experimental results.

This work results from a partnership between LIMATB and CEMUC aiming to analyse the deep drawing process of a cylindrical cup, corresponding to the first step of the Demeri test. The material used is an aluminium alloy AA5754-O which industry seeks due to its good mechanical properties. However, it is also characterized by presenting high springback values. This work analyses the effect of several parameters such as: (i) variation of die dimensions; (ii) influence of the contact with friction conditions; and (iii) influence of contact pressures in the production of cylindrical cups with ironing on the its wall. The analysis of these parameters is performed with the aid of numerical simulation and experimental tests.

The numerical simulations are performed using the in-house code DD3IMP, developed by CEMUC, and the experimental tests were performed at LIMATB laboratory. I order to better understand the influence of the parameters in study, this work provides an analysis of the forces involved in the process as well as the thickness distribution. The main conclusion are that the die has the most influence on the process, since its inner diameter limits the gap to the punch, and has the highest contact pressure on the contact

with the sheet. The results obtained by numerical simulation are confirmed by the experimental results.

Keywords: Deep Drawing, Numerical Simulation, Friction, Lubrication, Ironing, Springback, Die dimensions.

Contents

List of Figures

List of Tables

SYMBOLOGY AND ACRONYMS

Symbology

β – limit drawing ratio

D – initial blank diameter

d – drawn cup diameter

$r_0 + r_{45} + r_{90}$ – plastic anisotropy coefficients

$\bar{r}$ – average anisotropy coefficient

Δr – planar anisotropy coefficient

E – Young's modulus

υ – Poisson ratio

F, G, H, L, M, N – Hill'48 anisotropy criterion parameters

σ_{ij} – Normal components of the Cauchy stress tensor

$\bar{\varepsilon}^p$ – Equivalent plastic strain

Y_0, Y_{sat}, C_Y – Voce law material parameters

Y – Yield stress

Acronyms

AA5754-O – aluminium alloy 5754-O

Blank – Flat rolled sheet

DD3IMP – Deep Drawing 3d implicit code

PLC effect – Portevin-Le Châtelier

RD – Rolling Direction

TD – Transverse Direction

1. DEEP DRAWING PROCESS

Nowadays, most of metal products used in daily life are processed by sheet metal forming. This manufacturing process is used since the end of the 19th century and has been greatly improved until the present, since it allows producing the desired shape by a simple process. Unfortunately the harmful phenomenon of springback usually occurs after the deep drawing process, being the main reason of warping and change of shape of the final product. Numerical simulation of this forming process has an important role in process design and optimization, because it can help predicting the common defects such as splits, wrinkles, springback and material thinning.

This chapter starts by presenting the background of the study, which is mainly focused on the deep drawing of a cylindrical cup. Therefore, the following sections present a description of the phenomena usually present in the deep drawing processes, as well as a discussion about the type of forces that occur and the influence of some physical parameters on the process. The discussion presented in this chapter is based on the literature review.

1.1. Framework

This work results from a partnership between the LIMATB (Laboratoire d'Ingénierie des MATériaux de Bretagne) and the CEMUC, (Centro de Engenharia Mecânica da Universidade de Coimbra). The study focused on the analysis of numerical and experimental results of a sheet metal forming process performed with an aluminium alloy 5754-O (AA5754-O), which is a material used in automotive industry applications.

The use of this alloy in the automotive industry has been limited due to the surface defects that occur during the stamping process. Those defects do not allow employing the AA5754-O in exterior or visible parts. In the last years, the CEMUC and LIMATB laboratories have jointly developed several studies in order to better characterize the behaviour of this alloy in deep drawing processes. These studies introduced a good progress in the mechanical behaviour and deep drawing characterization of this alloy at room and warm temperature. It was found that, at warm temperature, some phenomena, as

the springback and the PLC effect (Portevin-Le Châtelier) are considerably lower [Park and Niewczas, 2008; Coër, 2009; Coër et al., 2010; Laurent et al 2008; Laurent et al., 2010; Laurent et al., 2011; Oliveira et al., 2011; Grèze, 2009].

In this work, the numerical simulations were performed using the in-house code DD3IMP produced and developed by CEMUC, and the experimental test were performed at LIMATB laboratory. This highlights the importance of this partnership to the study. Although integrated in a broader research, during this study the tools' dimensions, the lubricant conditions and contact conditions were analysed, to better understand their influence on the deep drawing of cylindrical cups.

1.2. Deep drawing process

According to DIN 8584-3, the deep drawing is a process in which a sheet metal blank is radially drawn into a forming die by the mechanical action of a punch [Wikipedia, 2012a]. This process allows obtaining a complex shape part through a simple process, based on the plastic deformation of the metallic sheet. Sheet metal forming is a high productivity manufacturing process that is largely used in industries such as the automotive and the machinery components, to produce products made from metallic flat rolled sheet (blank). This process involves three main tools, namely: punch, blank-holder and die. The die defines the shape of the product to be drawn. The punch is used to move the sheet into the die's cavity and deform the sheet to its final shape. The blank-holder presses the sheet against the die (typically using a constant force or gap), which prevents the wrinkling of the sheet and controls the sheet sliding during the drawing process.

In Figure 1 the deep drawing process is schematically shown for a cylindrical cup, which is the geometry used in this study. The figure shows the successive steps from an originally blank to the product with its final shape. In the first step the lubricant is applied on the sheet's surfaces. The second step corresponds to the blank-holder closured. During the third step the punch is moved down to deform the sheet to its final shape. Finally, the punch is pulled back and the blank-holder force is removed. Then, in the last step the sheet is removed from the die cavity.

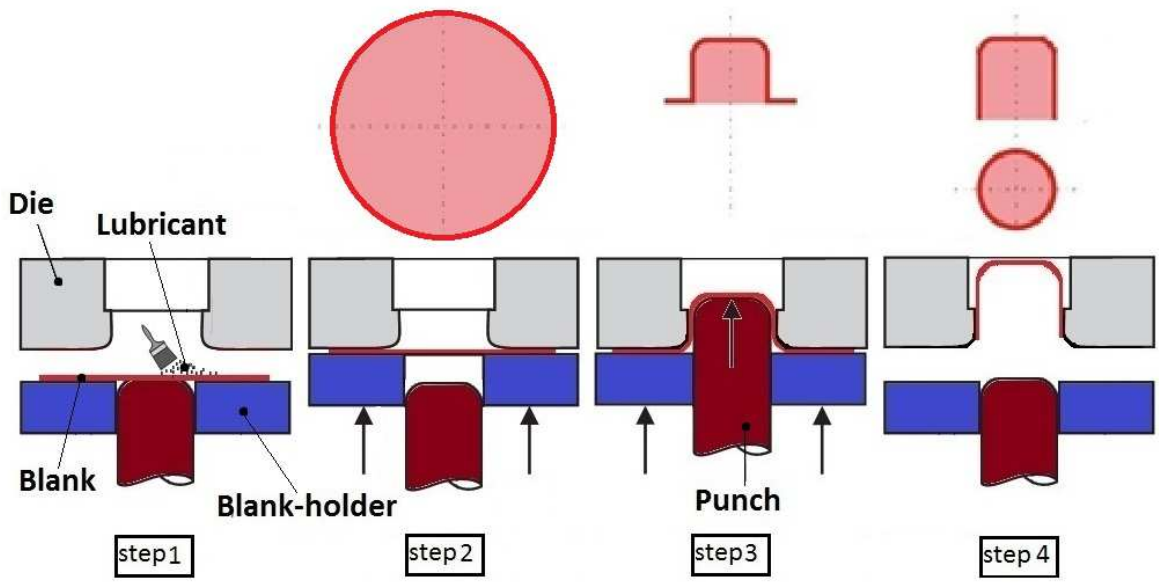

Figure 1 – Deep drawing process of a cylindrical cup.

In industry, after the last step the part usually undergoes other mechanical processes, namely trimming. In the trimming process, the excess metal that is necessary to draw the part is cut away from the finished part. Usually, during the last step of the forming process, the elastic recover of the material occurs, the so called springback. However, when trimming operations are also included in the process, springback also occurs due to the release of the residual stresses present in the part after the deep drawing operation. The springback phenomenon that occurs in the trimming operations usually contributes to the part warping, which is one of the surfaces defects that inhibits the service application of deep drawn parts.

1.3. Harmful phenomena in sheet metal processes

The two main problems regarding the application of the AA5754-O in autobody parts are the PLC effect and the springback phenomenon. Thus, over the last years several studies have been focused on the minimization of their effects during sheet metal processes. Recent studies have shown the potential advantages of warming forming processes in the reduction of both phenomena [Coër et al., 2010; Grèze 2009; Laurent et al., 2011]. In the following section these harmful phenomena are explained with more details.

1.3.1. Springback

The springback is measured as the difference between the final shape of the part and the shape of the forming die which, as previously mentioned, defines the part' shape at the end of the forming stage. Figure 2 shows an example of the different final shapes obtained after a deep drawing process, performed with the same tools and process conditions, using two blanks with different material properties, to better understand the importance of this phenomenon. This phenomenon plays an important role in process design, because wrong part dimensions is a problem to the assembly process, increasing the amount of scrape and, consequently, the part's cost. Nowadays the numerical prediction of the springback is still a research challenge, trying to achieve the required accuracy, necessary to be able to apply numerical strategies for its minimization. However, during the last years many studies have focused on this subject and, consequently, the numerical simulation has made significant progress. In this context, several tests have been proposed in order to better evaluate the springback phenomenon under different process conditions. For example, Demeri et. al. (2000) proposed a simple benchmark test that is often used to evaluate the springback.

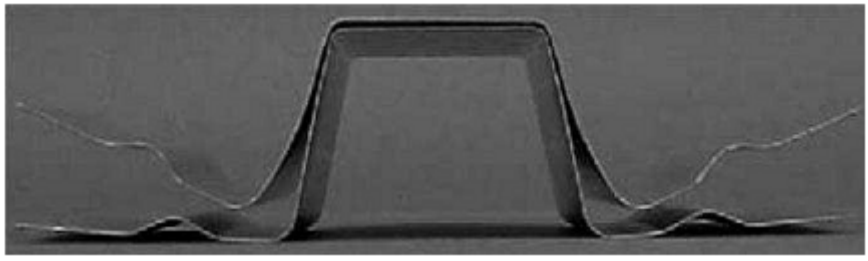

Figure 2 – Example of springback in a rail [Hsu et al, 2002].

1.3.1.1. Demeri test

The Demeri test, also called split-ring test, provides a simple benchmark for correlating the springback predicted by finite element analysis with experimental measurements. As showed in Figure 3, this test consists in cutting a ring specimen from a full drawn cup and then to split the ring longitudinally along a radial plane. The difference between the ring diameters, before and after splitting, gives a direct measure of the springback phenomenon, and indirectly, of the amount of residual stresses in the drawn cup [Demeri et al., 2000]. However, in this test it is important to take into account that the springback increases with the distance from the cup's bottom [Xia et al., 2004; Gnaeupel-

Herold et al., 2004]. The main reason for the springback phenomenon are the tangential stresses, perpendicular to the split plane, which are present in the cup due to the deep drawing process, as showed by Gnaeupel-Herold et al. (2004) for a carbon steel and by Grèze (2009) for the AA5744-O.

Figure 3 – Split- ring test, 1 – initial cup, 2 – split-ring, 3 – cup's bottom and top after the trimming of the ring.

1.3.2. PLC effect

The propagation of inhomogeneous plastic deformation bands is also known as PLC effect. It describes the serrations present in the stress-strain curve after the critical strain, which is the minimum strain needed for the onset of the serrations in the stress-strain curve [Wikipedia, 2012b]. This effect present in the 5000 series aluminium alloys is due to the magnesium atoms that block the dislocation movements [Boogaard,(2002; Halim, et al 2007]. It causes a drastic decrease of the material's plasticity and ductility's, and additionally a rough surface on the material that undergoes plastic deformation. This surface roughness developed during deformation makes the parts useless for autobody exterior parts. The temperature and strain rate (drawing speed) plays an important role to minimize this damaging phenomenon [Coër et al., 2010; Grèze, 2009; Halim, et al., 2007; Laurent et al., 2011].

1.4. Controlling sheet metal forming processes

In order to better understand the deep drawing process, namely how it is influenced by the main process parameters and the type of defects, it is necessary to know the forces and stress states that occur during the process. In the following sections some details about the force, stresses and process parameters will be briefly described, mainly focusing in the analysis of the deep drawing of cylindrical cups.

1.4.1. Forces

Figure 4 presents the force's distribution during a cylindrical cup deep drawing process. It is possible to see that the cup's bottom is the area less affected by the process conditions, being submitted only to compression, due to the punch's force. On the contrary, the bent and re-bent area near the cup's bottom is the more critical place, since it is typically place were fracture occurs. The flange is the area located between the die and the blank-holder. Note that when the sheet is moved into the die's cavity, the flange is strongly compressed in the circumferential direction while is being pulled in the radial direction. The circumferential compressive stresses result from the fact that the blank must reduce its radius in order to fit inside the die's cavity. The radius reduction is balance by a proportional increase of the cup's length, which depends of the material's hardening and anisotropic behaviour. The force exerted on the sheet by the punch, also called punch force, is directly connected to the material's mechanical properties, the blank-holder forces and the friction forces [Grèze, 2009; Westeneng, 2001; Özek and Bal, 2009].

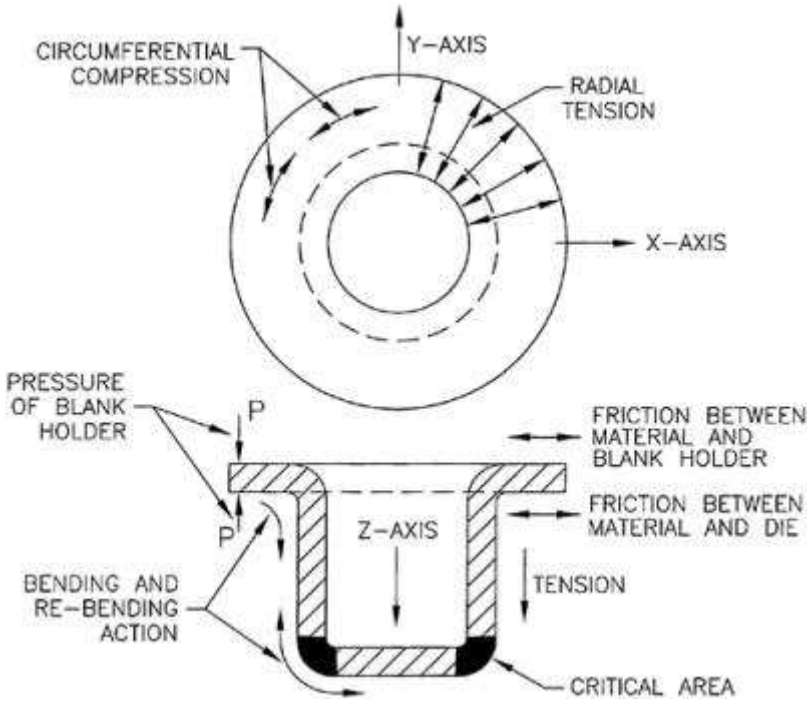

Figure 4 – Forces in the deep drawing process of a cylindrical cup [globalspec].

1.4.2. Influence of process parameters

The deep drawing depth can be interpreted as a technical obstacle for the deep drawing processes. Normally, it is indirectly defined by the limit drawing ratio β, which is also used to access the material formability. This corresponds to the ratio between the maximum initial sheet diameter, D, and the punch diameter , d, for a fully drawn cup, $\beta = D/d$. Therefore, in order to determine this value it is necessary to inspect the part to evaluate edge crack occurrence. When drawing cups for large drawing ratio values, larger radial tension is created on the flange and higher tensile stress is needed on cup wall [Özek and Bal, 2009; Grèze, 2009]. The stress state can be controlled by different process parameters. Therefore, the success of a cylindrical cup sheet metal forming process is directly linked with the deep drawing speed, blank-holder force, friction coefficient, temperature and tools geometry. The influence of each one of these parameters in the cylindrical cup deep drawing process is nowadays well known. However, it is important to note that they are all connected and sometimes the variation of one implies changing the others. All these parameters play an important role in the sheet metal forming, which will be briefly described in the following subsections. However, in this study only the tools geometry and the lubrication conditions will be analysed.

1.4.2.1. Tools geometry

The tools geometry is an important and difficult problem in sheet metal forming. As showed by Özek and Bal (2009), the limit drawing ratio and the residual stress are greatly linked with the tools geometry, particularly the shoulder radius. Their surface condition is also essential to reduce the friction and give a good appearance to the final part. The tools should not mark, damage or weaken the final part. Therefore, the absence of contours in the project parts can make easier the conception of the tools and the parts. Thus, a geometry study should be developed in function of the material used [Özek and Bal, 2009; Han, 1997].

1.4.2.2. Blank-holder forces

The main goal of using a blank-holder is to control the blank sheet flow and avoid wrinkling. A too high value for the blank-holder force leads to materials rupture, but a too low blank-holder force allows the sheet wrinkling. Therefore, it is of paramount importance to find the appropriate value for the blank-holder force. Higher values of blank-holder force also contribute for a higher punch force and reduce the thickness on the cup's wall [Grèze, 2009]. On the other hand, for higher blank-holder force values the springback phenomenon seems to decrease, due to the high values of plastic strain attained and to the thickness reduction, as reported for the ring open in the Demeri test example by Baptista et al. (2005) and Enchempati and Dev (2002). Nevertheless, as it is mentioned by Emmens (1997), when using a constant blank-holder force during deep drawing the pressure in the flange region increases due to the decreasing contact area. This increase of pressure can explain the previously mentioned increase of the springback with the increase of the distance to the cup's bottom in the Demeri test. In fact, the flange is strongly compressed in the circumferential direction while it is also being compressed in the thickness direction, which can lead to a gradient in the stress state along the cup's wall.

1.4.2.3. Temperature

Traditionally the deep drawing process takes place at room temperature. However, some researchers have focused their attention in exploring the influence of temperature in the mechanical properties of metallic sheets [Laurent et al., 2011; Manach et al, 2008]. In warm forming, the sheet metal is processed bellow the recrystallization temperature. For the AA5754-O, shear test results show that between 25º – 150º the yield

stress is not meaningfully changed [Coër et al., 2010; Grèze, 2009]. The temperature effects tend to decrease the stress gradient in the cup wall, which is directly linked to the decrease of the springback and stamping forces. This also permits to increase of the limit drawing ratio [Boogaard, and Huétink, 2006; Grèze, 2009; Manach et al., 2008]. The temperature increase activates the dislocation motion and dislocation-dislocation interactions that result in a viscosity decreases. For this alloy it is also observed that the PLC effect disappears for temperatures higher than 100º, because the temperature increases the freedom of the magnesium atoms, which block the dislocation movements at room temperature [Coër et al., 2010; Grèze, 2009].

1.4.2.4. Deep drawing speed

Deep drawing speed has a greater influence in the deformation process. The use of a high drawing speed can lead to rupture, but a slow speed is also not possible in industrial processes, because in industry time is money. This parameter is directly linked to the material's mechanical behaviour and, consequently, to the deep drawing forces. The strain rate sensitivity indicates if a material is sensitive to the strain rate or not. A material that shows the same stress-strain curve for increasing strain rates is say to present a null strain rate sensitivity. If the stress-strain levels increase with the strain rate the material presents positive strain rate sensitivity, otherwise is negative. Therefore, a material that presents positive strain rate sensitivity will present higher punch forces for higher punch speed. However, this characteristic can change with temperature. The quality of a deep drawing part is also linked with the PLC effect, which tends to decrease with the decrease of the drawing speed. Therefore the drawing speed should be chosen as a function of the nominal working conditions. The AA5754-O used in this work is slightly sensitive to the strain rate, as showed by Grèze (2009).

1.4.2.5. Friction

Friction is primarily connected with the contacting pair of materials and the lubricant conditions. Basically, higher punch force values are linked with higher global friction coefficient values. In fact, high friction coefficient values are dangerous to the drawing process, but the friction can be easily reduced through the use of a lubricant. Unfortunately, this parameter cannot be experimentally measured with the desired accuracy, because it changes with many conditions including the contact pressure and

sliding distance. The difficulties related with its accurate modelling result also from the fact that it is influenced by many parameters, including temperature, sliding velocity and the characteristics and amount of lubricant used. Although in the last years many researchers have focused their attention on trying to minimize the use of lubricants, typically deep drawing process involve lubricated contact conditions. [Figueiredo et al., 2011; Guillon et al., 2001; Magny, 2002; Westeneng, 2001]

1.5. Lubricant conditions evolution

The lubricant conditions play a key role in minimizing the tool's wear and in reducing the friction. Proper lubricant conditions reduce the formation of scratches on the sheet and also reduce the friction coefficient. However, the lubricant conditions depend from parameters like temperature, sliding velocity and pressure. These parameters have a greater influence in the fluid's viscosity and, consequently, in its elasto-hydrodynamic deformation. In order to better understand the friction's problem Figure 5 presents the so-called generalized Stribeck curve, where it is possible to distinguish the three different lubricant regimes.

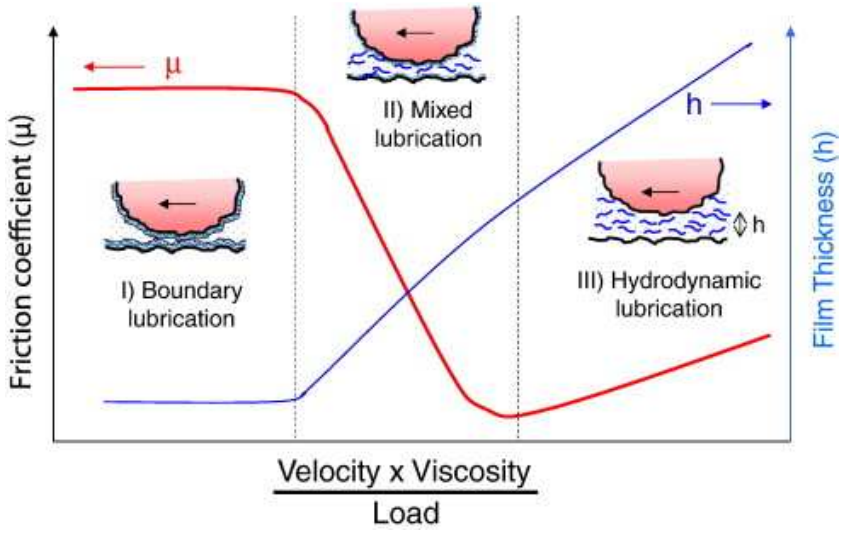

Figure 5 – Generalized Stribeck curve [Coles et al., 2010].

Boundary lubrication – The bodies come into closer contact at their raised solid features, called asperities, and the load is totally carried by them. These surfaces are protected from dry contact by thin boundary layers, which are attached to the surfaces.

Mixed lubrication – The opposing surfaces are separated by the film of lubricant. The load is shared between contacting asperities and lubricant.

Hydrodynamic lubrication – The contact between the surfaces does not occur and the load is carried totally by lubricant. The sliding depends on fluid's viscosity, which changes with temperature.

1.5.1. Contact regions evolution

Figure 6 schematically shows the most important contact regions of the deep drawing of a cylindrical cup. Schey (1983) identified the six different regions marked in Figure 6. The first region is located between the blank-holder and the sheet, and the second is between the die and the sheet. Together they are called flange region and the nominal pressure here is about ten times lower than in third region. This one characterizes the contact between the die radius's and the sheet. Here, the tension force is high and stretching play an important role. The fourth region corresponds to the contact between the punch flank and the sheet. In this region the sheet is stretched, although no real contact occurs. The contact between the punch radius and the sheet occurs in fifth region where the tension force also attains high values. The sixth and last region describes the contact between the punch's bottom and the sheet. In this region the sheet is mainly subjected to stretching [Schey, 1983].

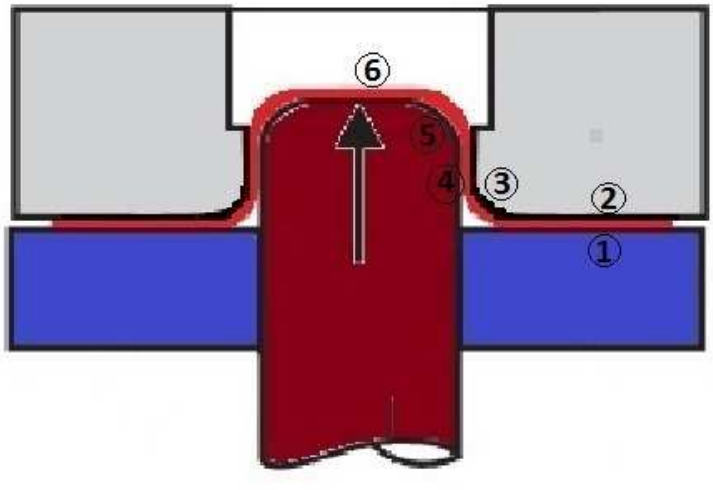

Figure 6 – Contact regions on the deep drawing of a cylindrical cup process, according to Schey (1983).

Regions 6 and 4 do not have a great influence in the deep drawing process. The friction in region 5 must be sufficiently high to ensure that the sheet follows the punch

movement. On the other hand, the friction in regions 1, 2 and 3 must not be too high, because a high friction leads to higher punch forces, resulting more easily in fracture [Westeneng, 2001].

As mentioned by Westeneng (2001), it is possible to consider that the flange region (regions 1 and 2 in Figure 6) are typically in the Mixed-Boundary lubrication condition and that the areas corresponding to the die and the punch radius's (regions 3 and 5 in Figure 6) are only in Boundary lubrication condition, due to the high contact pressures developed.

1.5.2. Influence of sliding direction on lubrication

The roughness has a great influence on the lubrication regime. The roughness depends on the manufacturing process. In the case of the blank, obtained by rolling process, the roughness surface is like waves parallel to rolling direction (RD), but for the tools is not the same and depends of the machining process [Roizard et al., 1999]. Roizard et al. (1999) also describe the influence of the roughness orientation of the sheet on the friction. It was observed that for 0º to RD the friction is not affected by the increase of the sliding speed. However, for TD is possible to observe that an increase of the sliding speed causes a decrease of the friction value. This influence of the sliding speed with the angle to the RD is due to the channels developed during the rolling manufacturing processes, which are parallel to RD. As explained by Roizard et al. (1999) for the transverse sliding the lubricant is locked by the ridges (micro-hydrodynamic bearing), and for the parallel sliding the lubricant can flow easily along the roughness channels (no micro-hydrodynamic bearing).

1.6. Summary

In this chapter a review of the deep drawing was presented, focusing the main problems and the approaches used to control this forming process. The main problems concerning the extended application of the AA5754-O in the industry were presented, highlighting the problems related with springback and PLC phenomena. Today, they constitute main weakness for applying forming processes to 5000 series aluminium alloys

.

After of one brief presentation of the deep drawing process and its problems, the influence of process parameters on the forces acting during the process was discussed, as well as their influence on the deep drawing of cylindrical cups. One of the more important process parameters is the friction, which depends on the lubricant conditions. Therefore, some details about the evolution of the lubricant conditions were also presented.

2. EXPERIMENTAL AND NUMERICAL PROCEDURE

The goal of this chapter is to present the details concerning the experimental and numerical procedures used in this study. First the material composition is presented, as well as some results obtained from its mechanical characterization. After that the experimental procedure and its different steps are described, followed by a description of the experimental results acquired and analysed. Nowadays, numerical simulation of forming processes, with the finite element method, is often used in order to better understand the influence of the material and process parameters during the deep drawing processes, and particularly their interactions. This was also the procedure adopted in this work. In this chapter, the model adopted in the finite element simulation is detailed, including the constitutive model, the blank sheet discretization, the tools modelling and the friction law adopted.

2.1. Material Properties

The base material for the deep drawing of the cylindrical cup is an aluminium blank. The aluminium alloy selected is often used in automotive industry applications, such as inner door panels. The AA5754-O is manufactured by rolling operations and its composition in weight is presented in Table 1.

Table 1- Composition in weight % of AA5754-O.

Cu	Mn	Mg	Si	Fe	Cr	Al
≤0.10	≤0.50	2.60-3.60	≤0.40	≤0.40	≤0.30	93.6-97.3

The mechanical properties of this alloy were evaluated by performing tensile and shear tests. The results given by these tests are used to determine the material parameters of the constitutive model selected for the numerical simulation. The orthotropic behaviour can be determined based on the monotonous tensile tests carried out at 0° (rolling direction, RD), 45º and 90º (transverse direction, TD), from the rolling direction of

the sheet. The PLC effect is presented in this alloy and is characterized for some oscillations in the stress-strain curves at room temperature. The plastic anisotropy coefficients were determined by fitting the results of the plastic strain in width versus the plastic strain in thickness up to 0.20 of longitudinal strain The average anisotropy coefficient is expressed by the law $\bar{r} = (r_0 + r_{45} + r_{90})/4 = 0.765$ and the planar anisotropy coefficient is obtained by $\Delta r = (r_0 + r_{45} + r_{90})/2 = -0.170$. The shear tests were performed with an apparatus consisted of a Shimadzu AG-50kNG instrument adapted for shear testing [Coër et al., 2010; Grèze, 2009; Oliveira et al., 2011].

2.2. Experimental procedure

The experimental tests were performed in a Zwick/Roell-BUP200 machine presented in Figure 7. The control parameters are the drawing speed, the holding force and the maximal punch displacement. The experimental tests were performed using a deep drawing speed of 1mm/s and a blank-holder force of 6kN, at room temperature. The drawing force as a function of the punch displacement was recorded for all tests.

Figure 7 – Zwick/Roell-BUP200 machine.

The tools involved in the process are presented in Figure 8. In the process under analysis there is also a new tool, the ejector, with the function of removing the cup

from the die cavity after the punch displacement. This tool has no effect on the cup's deformation and that is the reason why it is rarely mentioned in the text. Figure 8 a) presents the tools used in the experimental tests and the Figure 8 b) presents a 2D sketch with its main dimensions.

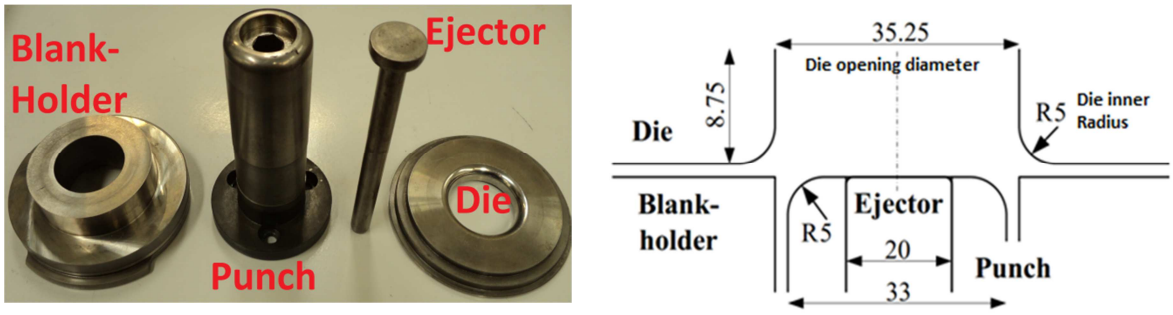

a) b)

Figure 8 – a) Tools used in experimental tests; b) 2D tool's sketch with the main dimensions.

The experimental procedure can be abridged to the four steps showed in Figure 1. However, it is important to detail the tasks associated with the first step:

1) Cut a circular blank with a 60 mm radius;
2) Measure the blank weight 6 times;
3) Spread uniformly the lubricant on the blank surface by the aid of a soft roll;
4) Measure again the blank weight 6 times;
5) Measure the blank-holder weight 6 times;
6) Spread uniformly the lubricant on the blank-holder surface by the aid of a soft roll;
7) Measure again the blank-holder weight 6 times.

The aim of the weight measure is to quantify the amount of lubricant used, given in g/m^2, in order to study the influence of the amount of lubricant used in the deep drawing process. Figure 9 presents four pictures showing different amounts of oil on the sheet and on the blank-holder surface's. These pictures give an idea of how the oil is spread in the sheet and blank-holder surfaces. For the experimental procedure detailed in this work, it was decided not to use lubricant on the punch , since it is impossible to quantify the amount of lubricant.

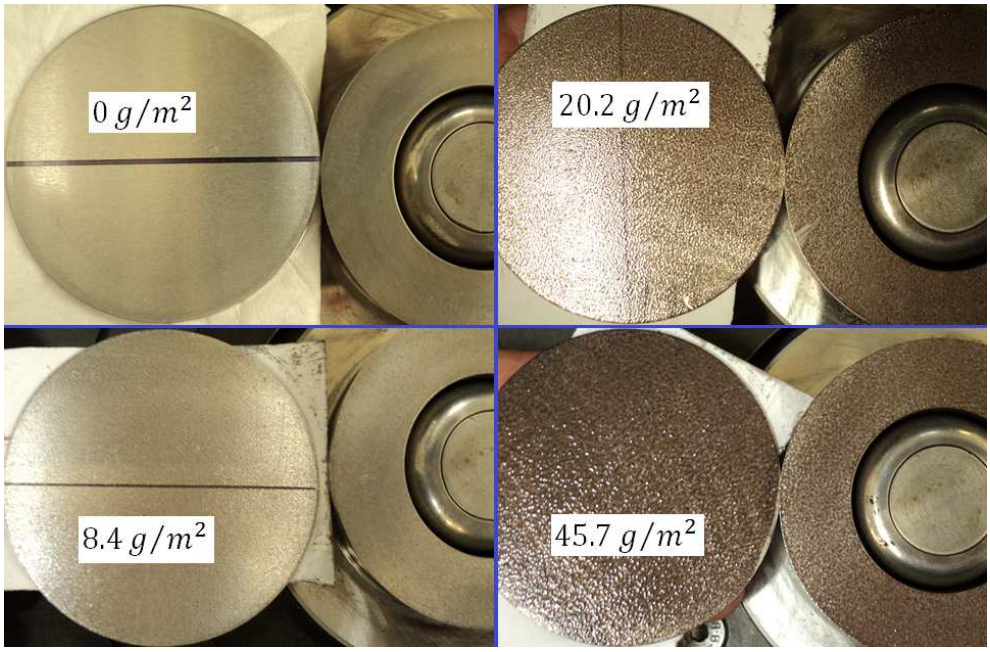

Figure 9 – Oil distribution on the sheet and blank-holder surface's for different amounts of lubricant, indicated in g/m$^{2.}$

The lubricant used is an JELT oil (Graisse Hautes Températures) with a viscosity of 96cSt at 40°C. More details about this oil can be found in annex. The weighing-machines used are a Sartorius BP210S and a Sartorius BP4100S. The first one is used to measure the sheet weight and has an accuracy of ±0.0001g and a maximal weight of 210g. The second one is used to measure the blank-holder. Its accuracy is ±0.01g and its maximal weight is 4100g. The average sheet's weight is 7,5717g, and average blank-holder's weight is 780.63g. The difference on the accuracy of the weighing-machine is justified by the relative error. The relative error is the absolute error (accuracy) divided by the magnitude of the exact value and expressed in terms of percentage, which is about 0.0026% for these measurements.

2.2.1. Punch force evolution

Figure 10 presents the punch force evolution in function of the punch displacement, for a test performed at room temperature with a blank-holder force of 6kN. In this figure it is possible to identify two different stages. The first stage corresponds to the common evolution of the punch force for a cylindrical cup deep drawing. In this stage the punch force increases until a maximum value of approximately 18kN, for a punch displacement of approximately 11 mm. Typically, after this punch displacement, the force

decreases until it reaches a null value. However, in this case at about 20mm of punch displacement a second stage starts, which is characterized by a sudden increase of the punch force. In this stage, after this sudden increase, the punch force continues to increase until attaining a maximum value for approximately 24 mm. Afterwards, the punch force decreases again until the end of the punch displacement.

The second stage of punch force increase occurs associated to the ironing process. In fact, during the deep drawing process there is an increase of the blank thickness for the material located between the die and the blank holder. Since the blank thickness is higher than the gap between the die and the punch, when this material reaches this location, a sudden increase of the punch force occurs.

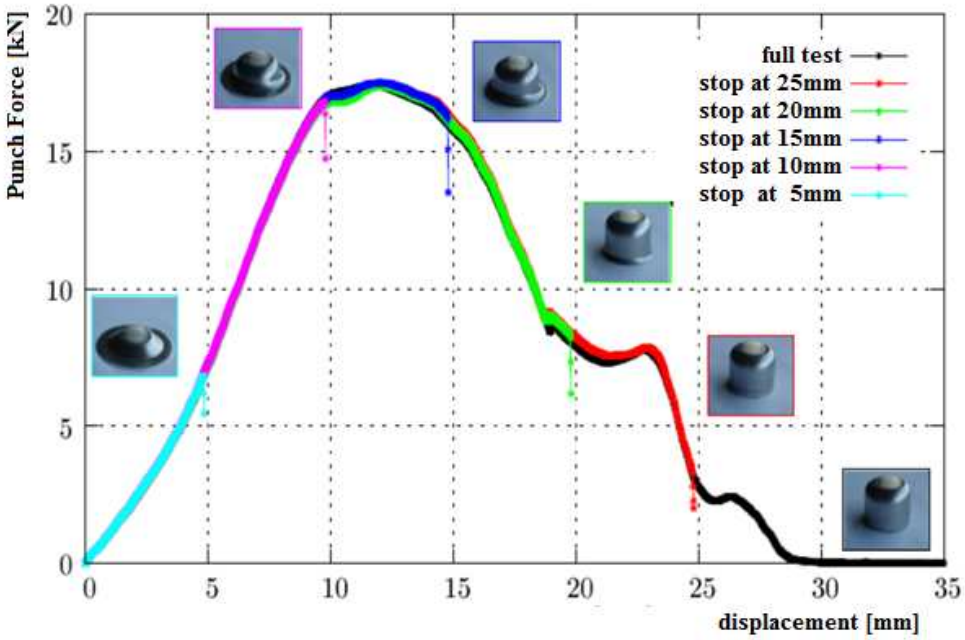

Figure 10 – Punch force evolution with the punch displacement.

2.2.2. Thickness evolution

The cup thickness' is analysed using a "Brown&Sharpe®" model "MicroXcel PFX-454" 3D measurement machine. The coordinates are given a Cartesian referential "X,Y,Z" along the directions at 0º; 45º; 90º; 135º; 180º; 225º; 270º; 315º to the RD, with a precision less than 0.010mm . The referential centre is coincident with the blank's centre. Although the measures are taken for all these directions, due to the cup's symmetry an

average of the different coordinates is performed in order to obtain the average evolution along 0º (average of 0º and 180º); 45º (average of 45º, 135º, 225º and 315º); 90º (average of 90º and 180º) to the RD. This average permits also a comparison of the experimental thickness results with the numerical ones, since the numerical model considered only a quarter of the cup's geometry. Also, by considering the average values it is possible to compensate for the small deviation of the cup's centre in the measuring machine. The Cartesian coordinates are later converted to spherical coordinates in order to calculate a curvilinear coordinate to analyse the thickness evolution with the distance from the blank's centre, along the different directions. This curvilinear coordinate is the one used to present the results.

The thickness evolution at the end of the cup forming is presented in Figure 11 along the RD. The distance corresponds to the curvilinear coordinate, which is measured from the blank's centre. It is possible to see that at the cup's bottom the thickness is almost constant with an approximate value of 1mm, equal to the sheet initial thickness. In the transition area, between the cup's bottom and the wall (i.e. Re-bending area), the thickness attains its minimum value. The critical areas occurs in the Re-bending area and in the begin of the cup's wall, and is usual associated to the rupture zone. After the Re-Bending area the thickness increases in the cup's wall until attaining the ears zone. In the ears zone the thickness keep its value almost constant. This is due to the ironing process that occurs in the material located in this area. Therefore, in this zone the thickness is equal to the value of the gap between the punch and the die.

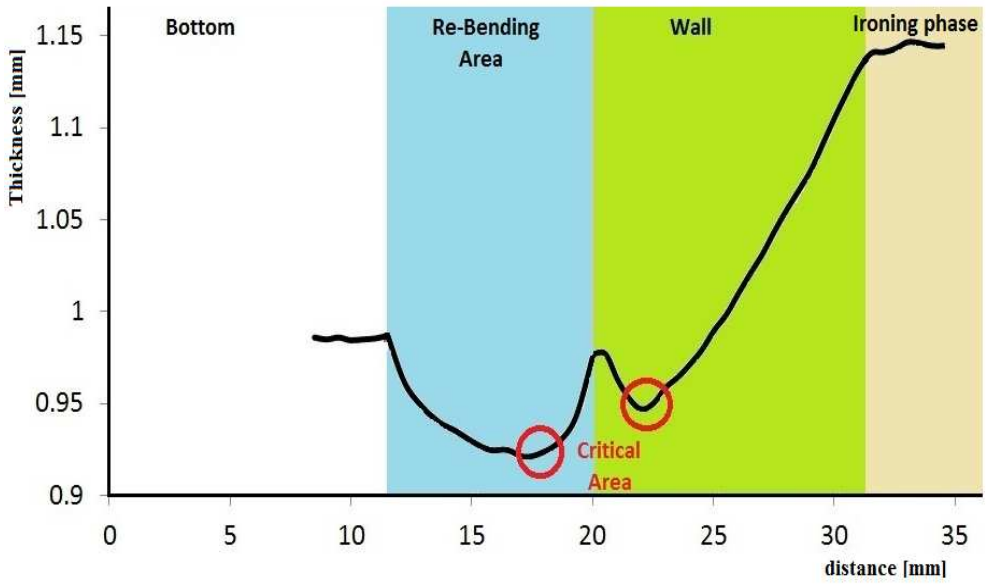

Figure 11 – Thickness evolution measured from the blank's centre along the RD.

2.3. Numerical Simulation

Finite element numerical simulation plays an important role in the prediction of phenomena as splits, wrinkles, springback and material warping. This technology allows the sheet metal part designers to quickly assess alternative designs, in order to optimize the part. It uses a model of the process and of the material's properties (constitutive model) to simulate the sheet metal forming process, by applying the non-linear finite element analysis. Its benefits in the manufacturing industry are unquestionable. It permits to shorten the lead times, cost and lean manufacturing, which are critical to the company success.

In this work the in-house code DD3IMP from DD3 (Deep Drawing 3D) family, is used to perform the numerical simulation. The following sections describe the constitutive model used in the simulation process as well as the blank sheet discretization, tools modelling and the friction law used. The material and numerical parameters used were previously studied, and are not the aim of this study [Coër, (2009); Coër et al., 2010; Grèze, 2009; Laurent et al., 2010; and Oliveira et al., 2011].

The numerical tests were performed considering the constitutive parameters determined based on the experimental test results previously mentioned, which are kept during the study. The blank-holder is controlled with a constant force of 6kN, the same

value used in the experimental tests. The parameters changed during the numerical study were the tools geometry and the contact conditions.

2.3.1. Constitutive model

The constitutive model is used in the numerical simulation to describe the material's mechanical behaviour during the drawing process. The mechanical behaviour is slip in two main regimes, the elastic and the plastic. This study assumes an isotropic behaviour during the elastic regime, described by the Young's modulus, E=70.4GPa, and the Poisson ratio, $\upsilon = 0.33$ [Oliveira et al., 2011].

The yield criterion gives the stress value at which a material begins to deform plastically. In this study the anisotropic Hill'48 yield criterion is used, which is given by:

$$F(\sigma_{yy} - \sigma_{zz})^2 + G(\sigma_{zz} - \sigma_{xx})^2 + H(\sigma_{xx} - \sigma_{yy})^2 + 2L\sigma_{yz} + 2M\sigma_{zx} + 2N\sigma_{xy} = Y^2, \quad (2.1)$$

the coefficients F, G, H, L, M and N are the anisotropy parameter and are presented in the Table 2. This parameters were identified using the classical relationship between them and the parameters r_0, r_{45} and r_{90}, determined from the tensile test results. Note that for the parameters $F = G = H = 0.5$ and $M = N = 1.5$ this criterion becomes the isotropic von Mises yield criterion.

The plastic behaviour is also described by a work hardening law and an associated flow rule. The work hardening behaviour is modelled by the Voce law, given by:

$$Y(\bar{\varepsilon}^p) = Y_0 + (Y_{sat} - Y_0)[1 - \exp(-C_Y \bar{\varepsilon}^p)], \quad (2.2)$$

where Y_0, Y_{sat} and C_Y are the material parameters presented in the Table 2.

The results of the stress-strain curves from tensile and shear tests in the RD give the database for determining the work materials hardening law parameters with DD3MAT in-house code. The kinematic work hardening laws was not taken into account in this study due to the type of experimental results available and because it is not considered to be so important in the cylindrical cup deep drawing and ironing too.

Table 2 – Hill'48 and Voce law parameters for the AA5754-O.

Hill'48 parameters					**Voce Law**		
F	G	H	N	L=M	Y_0	Y_{SAT}	C_Y
0.5548	0.606	0.3939	1.5672	1.500	113.64MPA	292.83MPA	14.94

In the numerical simulations performed with DD3IMP in-house code, the contact with friction conditions are described using the Coulomb's law. The friction coefficient can be considered to be constant and equal in all tools or constant with different values for each tool.

2.3.2. Tools modelling and blank sheet discretization

These parameters have been previously analysed by Laurent et al. (2010) and Oliveira et al. (2011), which are the basis to the numerical simulations performed during this study.

The numerical model considers the four tools: die, blank-holder, punch and ejector. The first one is modelled using Nagata surfaces and the others are modelled using Bézier surfaces, but all tolls are assumed to behave rigidly. Due to the geometrical and material symmetry only one quarter of the global structure is modelled.

The blank-holder applies a constant force of 6 kN on the blank surface and can move freely until establishes contact with the die, this provides a good correlation between the experimental test and numerical simulation.

The blank geometry is a circular sheet with 30 mm of radius and it is discretized with 3-D solid elements with 8 nodes (see Figure 12), which are integrated using a selective reduced technique. The size of the finite element along the radial direction is approximately 0.5 mm and is determined taking into account the die radius, in order to assure an accurate prediction of the punch force evolution. For the thickness, it is chosen to use three layers of finite elements. Previous studies indicate that this discretization keeps a good ratio between computational time and accuracy in the thickness prediction [Oliveira et al., 2011].

The ejector and the punch present a flat geometry, thus the central part of the blank is always discretized with a coarser finite element mesh, because it not expected that this zone will have an influence on the numerical results.

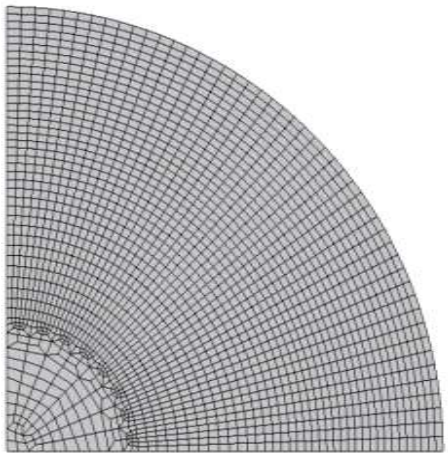

Figure 12 – Blank discretization, with 5976 elements and 8626 nodes [Oliveira et al., 2011].

2.1. Summary

In this chapter the numerical and the experimental procedure used in the study were presented. The analysis of a typical example of the punch force evolution with its displacement is performed, in order identify the two different stages. The first stage corresponds to the common evolution of the punch force during a circular cup drawing operation and the second stage occurs associated to the ironing phase of the process. The cup thickness' was also analysed highlighting the occurrence of the ironing process.

In the section devoted to the numerical procedure, the constitutive model parameters (Voce law to the work hardening behaviour and Hill'48 yield criterion) used as well as the blank sheet discretization, tools modelling and the friction law used are described.

3. NUMERICAL ANALYSIS

Numerical simulation of forming process plays an important role in the prediction of phenomena as splits, wrinkles, springback and material warping. In this study the in-house code DD3IMP was used to perform the numerical simulation of the circular cup deep drawing, in order to better understand the influence of the parameters in study during the deep drawing processes, and particularly their interactions. This chapter presents a numerical study about first, the influence of the tools dimensions and secondly, the influence of the friction conditions in the deep drawing processes.

For the first study, the die was selected for the analysis of tools geometry, since it can be considered has the tool with more impact in the overall final geometry. In fact, its dimension dictates the gap with the punch and the bending/unbending of the material. Therefore, this study focuses exclusively on the variation of the die dimensions. The dimensions under analysis are the "Inner Die Radius" and the "Die Opening Diameter". However, in the second study about the friction conditions effect on the forming conditions all the tools were considered, except the ejector. Based on the results obtained in the tools dimensions study, the different dimensions of the "Die Opening Diameter" are also varied in the friction conditions study.

Table 3 presents a description of the set of simulations carried out in both numerical studies. The labels selected for the tests are also presented in Table 3. For example, in the label “D35.25_R5.00”, the letter “D” is followed by the "Die Opening Diameter" value and the letter “R” by the "Inner Die Radius". In the label, “D35.25_F0.09”, the letter “F” is followed by the global friction value. The prefix “ISO” is used to identify the numerical simulations performed considering the von Mises isotropic model, in order to differentiate from all the other simulations that where performed with the Hill’48 anisotropic yield criteria. The label of type “D0P0BH9” is used only for models that considered different values for the friction coefficient for each tool. In these cases, the letter “D” represents the die, “P” the punch and the letters “BH” represent the blank-holder. Each group of letters is followed by the friction coefficient value used in the model. For example, the model with a die with a friction value of 0.09 is presented by D9. The

analysis of the influence of different friction for each tool is performed considering the original tool dimensions presented in Figure 8 b).

Table 3 – Numerical tests.

Name	Friction coef. on Die	Friction coef. on B-H	Friction coef. on Punch	Die opening Diameter (mm)	Gap between Die - Punch	Inner Die Radius (mm)	others
D35.20_R4.975	0.06			35.200	1.1	4.975	Different dimension for tool
D35.20_R5.000						5.000	
D35.20_R5.025						5.025	
D35.25_R4.975				35.250	1.125	4.975	
D35.25_R5.000						5.000	
D35.25_R5.025						5.0250	
D35.30_R4.975				35.300	1.15	4.975	
D35.30_R5.000						5.000	
D35.30_R5.025						5.025	
D35.20_F0.00	0.00			35.200	1.1	5.000	Anisotropic model
D35.20_F0.03	0.03						
D35.20_F0.06	0.06						
D35.20_F0.09	0.09						
D35.25_F0.00	0.00			35.250	1.125		
D35.25_F0.03	0.03						
D35.25_F0.06	0.06						
D35.25_F0.09	0.09						
D35.30_F0.00	0.00			35.300	1.15		
D35.30_F0.03	0.03						
D35.30_F0.06	0.06						
D35.30_F0.09	0.09						
D35.20_F0.00ISO	0.00			35.200	1.1		Isotropic model
D35.20_F0.03ISO	0.03						
D35.20_F0.06ISO	0.06						
D35.20_F0.09ISO	0.09						
D35.25_F0.00ISO	0.00			35.250	1.125		
D35.25_F0.03ISO	0.03						
D35.25_F0.06ISO	0.06						
D35.25_F0.09ISO	0.09						
D35.30_F0.00ISO	0.00			35.300	1.15		
D35.30_F0.03ISO	0.03						
D35.30_F0.06ISO	0.06						
D35.30_F0.09ISO	0.09						
D0P0BH9	0.00	0.00	0.09	35.250	1.125		Diff friction for tool
D0P9BH0	0.00	0.09	0.00				
D9P0BH0	0.09	0.00	0.00				

3.1. Effect of die dimensions

In the experimental study, there is always some uncertainty concerning the exact dimensions of the tools. This uncertainty can be derived from manufacturing errors, measurement errors or from the tool's wear. However in the numerical simulation, the tools are geometrically perfect and present no dimensional defects. Therefore, it is possible that the uncertainty in the tools dimensions may cause some divergence between the experimental and simulation results. In order to study the influence of a small variation in the tools dimensions in the predicted results, a set of simulations was performed. In the example under analysis, the die can be considered has the tool with more impact in the overall final geometry, since its dimension dictate the gap with the punch and the bending/unbending of the material. Therefore, the study focuses exclusively on the variation of the die dimensions.

The dimensions under analysis are the "Inner Die Radius" and the "Die Opening Diameter". The simulations were all performed assuming a friction coefficient of 0.06. Figure 8 b) presents the predefined die dimensions, which were changed 0,025mm in the inner radius and 0,050mm in the opening diameter of the die. It is important to note that, a change of 0,050mm in the die opening diameter correspond to a change 0,025mm in the gap between the die and the punch.

The green filled region in Table 3 presents the different combinations of the die dimension considered in the study. The idea is to consider the separated influence of the two design variables and also explore eventual interactions between them. Therefore, three different "Die Opening Diameter" were considered: 35.20mm; 35.25mm; 35.30mm and for each one the "Inner Die Radius" assumed also three different values: 4.975mm; 5.000mm; 5.025. The combination of these two variables, with three levels, results in nine different dies. It is important to note that the gap between the die and the punch change for the different "Die Opening Diameter" but it is not affected by the "Inner Die Radius", as highlighted in Table 3.

3.1.1. Punch force evolution with the punch displacement

In Figure 10 the punch force evolution acquired during the experimental deep drawing process was described and two different stages were identified. Figure 13 and

Figure 14 present the results obtained by the numerical simulation. According with these results, the die geometry only influences the ironing stage. It is possible to observe that the punch force increases in the ironing stage for smaller “Die Opening Diameter”. However, the punch force evolution is not affected by the “Inner Die Radius”. The difference in the punch forces evolution in the second stage is explained by the change in the gap between the die and the punch, induced by the change in the “Die Opening Diameter”.

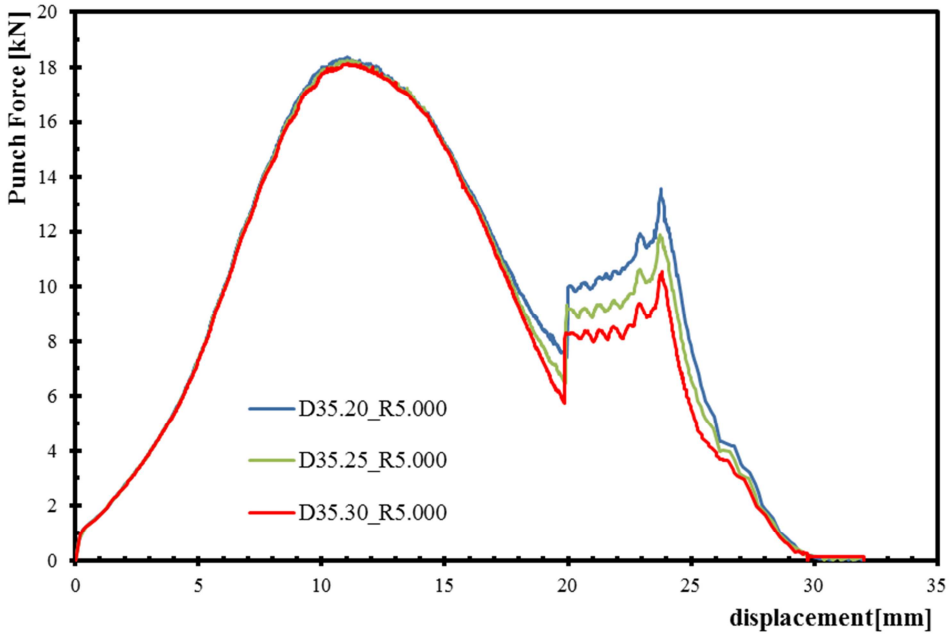

Figure 13 – Punch force evolution with the punch displacement, for the different “Die Opening Diameter”.

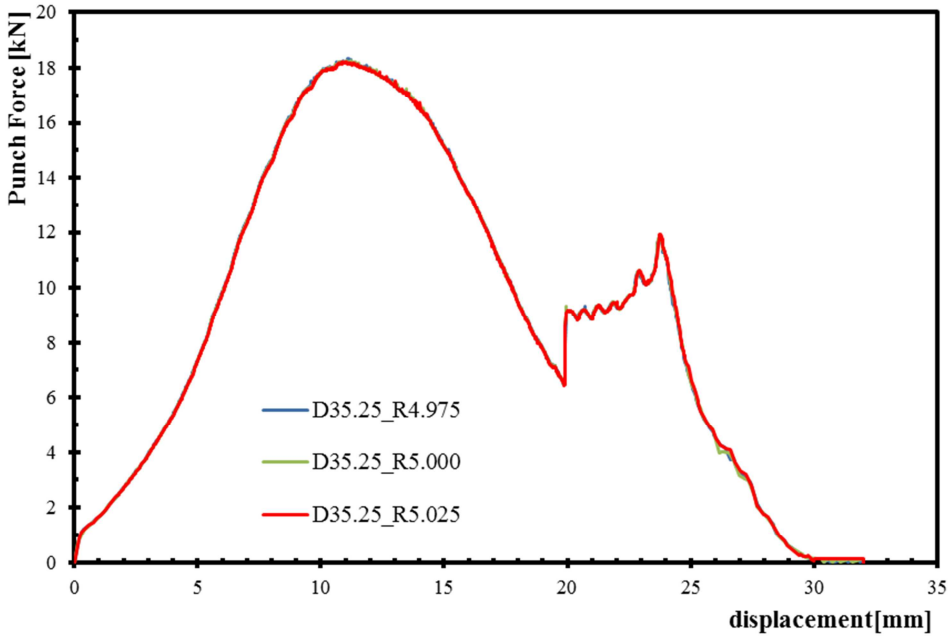

Figure 14 – Punch force evolution with the punch displacement, for the different "Inner Die Radius".

3.1.2. Thickness evolution

The thickness distribution at the end of the cup forming is presented in Figure 15 and Figure 16, along the RD. As for the punch force evolution, it is possible to confirm from Figure 15 that the increase of the die diameter results in an increase of the thickness in the end of the cup's wall. This is directly related with the increase of the gap between the punch and the die with the increase of the "Die Opening Diameter". Therefore, for a higher die diameter the ironing process is not so severe, which leads to higher thickness values in the cup's wall and smaller ironing punch forces (see Figure 13 and Figure 14). However, as shown in Figure 16, the thickness variation is not affected by the "Inner Die Radius". Note that, according with the Table 3 these geometries correspond to a constant gap of 1.125mm.

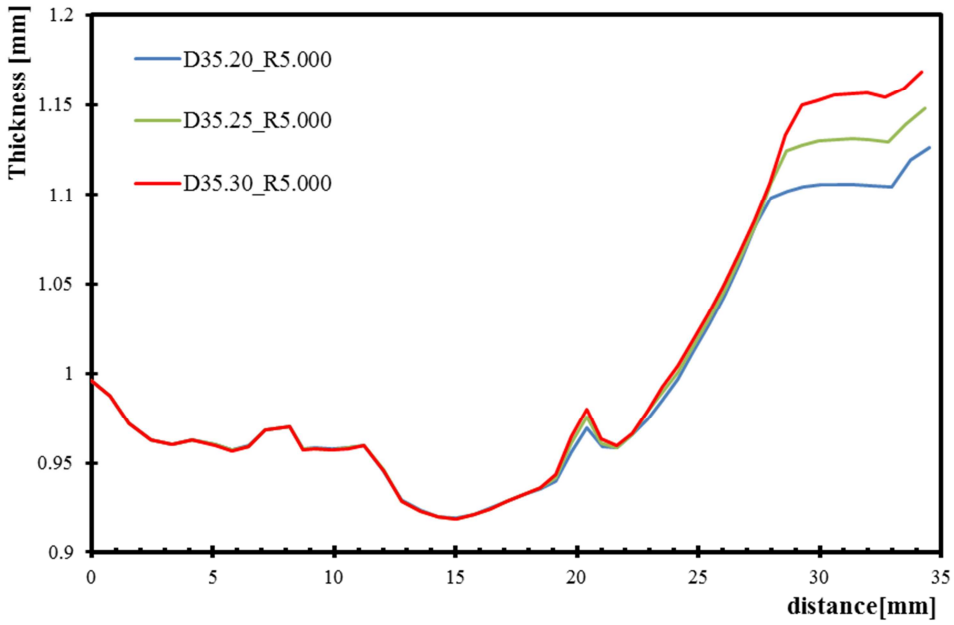

Figure 15 – Thickness evolution with the distance to blank's centre, along the RD, for the different "Die Opening Diameter".

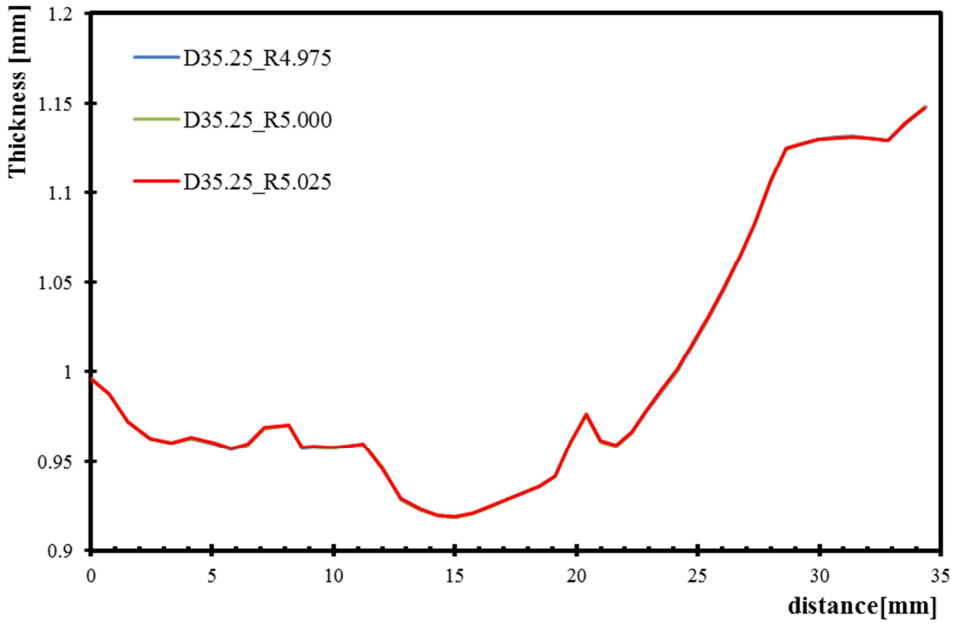

Figure 16 – Thickness evolution with the distance to blank's centre, along the RD, for the different "Inner Die Radius".

In order to analyse the effect of the die's diameter on the stamping process, a comparison of the thickness evolution for a 20 mm punch's displacement is presented in Figure 17. According to the punch force evolution curves showed in the previous section,

this value of punch displacement corresponds to the beginning of the ironing stage. It is notable that for this punch displacement the die geometry presents a negligible effect in the thickness evolution along the cup's wall. This confirms that before the starting of the ironing phase, the die diameter variation has no effect on the thickness evolution along the cup's wall. The result obtained with the die opening radius of 35.20 mm presents a smaller thickness value for about 30 mm from the blank's centre, which can be related with the begin of the ironing process.

Figure 18 presents the comparison of the thickness evolution for different punch displacements. It is noticeable the thickness reduction that occurs during the ironing process. Also, the ironing process does not cause any thickness variations on the sheet zones that have already pass the zone located between the die and the punch, it only affects the part of the sheet that goes through this zone. The strong increase of the thickness in the flange area between 16mm and 20mm of punch displacement can be explained by the strong circumferential compressing forces that occur in the flange area, due to the constant blank-holder force which starts to push the sheet to the inner die radius.

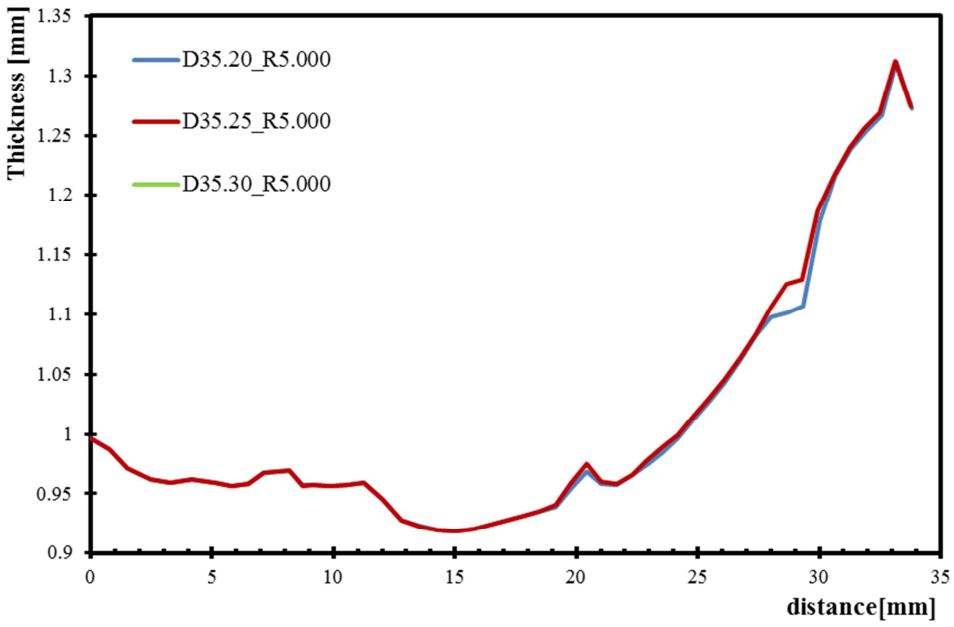

Figure 17 – Thickness evolution with the distance to blank's centre, along the RD, for the different "Die Opening Diameter" and 20 mm of punch displacement.

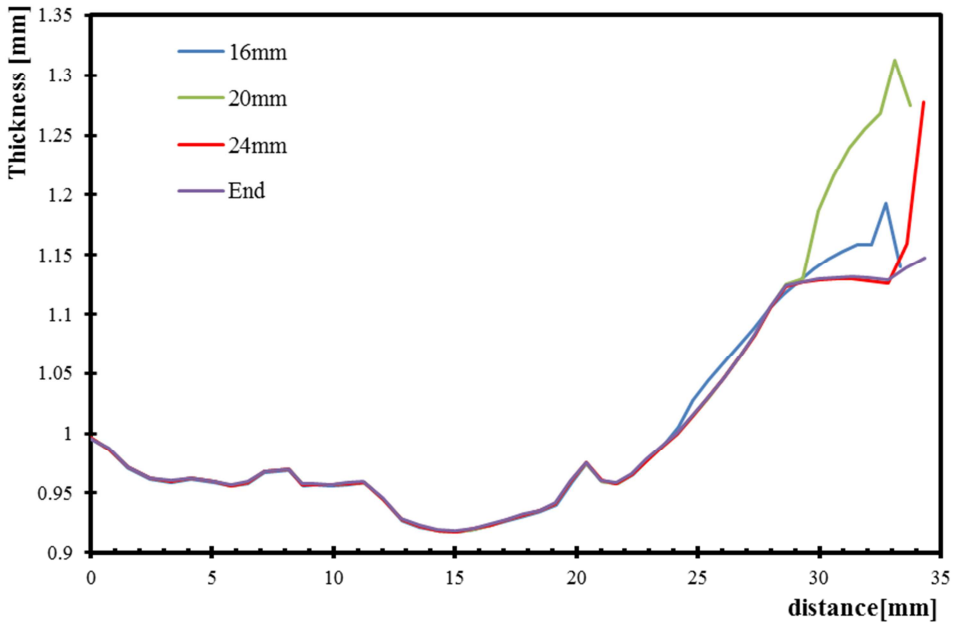

Figure 18 – Thickness evolution with the distance to blank's centre, along the RD, for different punch displacements, considering the same die.

3.2. Effect of friction conditions

In the second chapter an introduction to the influence of the friction in the deep drawing process was presented, as well as some details about the high influence of the lubricant conditions. In this section, the results of several numerical tests considering different friction conditions are presented, in order to better understand the influence of this parameter. Table 3 presents a resume of all the tests performed.

It is important to note that the numerical results presented in this section always consider the original tools dimension, presented in Figure 8 b), and the tools wear is not taken into account.

3.2.1. Global friction coefficient

The friction is a parameter often impossible to quantify in the experimental tests, but that plays a very important role in deep drawing process. With the purpose of analysing the influence of this parameter, numerical tests with different friction coefficient global values were performed. In Figure 19 to Figure 22, the result of these tests are presented to the friction values of 0,00; 0,03; 0,06 and 0,09. These tests were performed

considering the anisotropic behaviour of the material (Figure 19 and Figure 21) and isotropic behaviour (Figure 20 and Figure 22).

Figure 19 and Figure 20 present the punch force evolution with the punch displacement, considering anisotropic and isotropic behaviour of the blank, respectively. Both figures show an increase of the punch force with the increase of the global friction value, in both phase of the process, as expected. Figure 20 shows some oscillations in the predicted punch force evolution due to the relation between the blank discretization and the isotropic behaviour of the material. Globally, there is always a surface layer of nodes entering or leaving contact with the tools, leading to a globally smoother evolution, presenting more oscillations. Figure 21 and Figure 22 present the thickness evolution in function of the distance to the cup's centre, along of RD. Both figures show a small increase of the thickness with the decrease of the global friction coefficient value. This increase in the thickness is more evident in the cup's wall and re-bending areas.

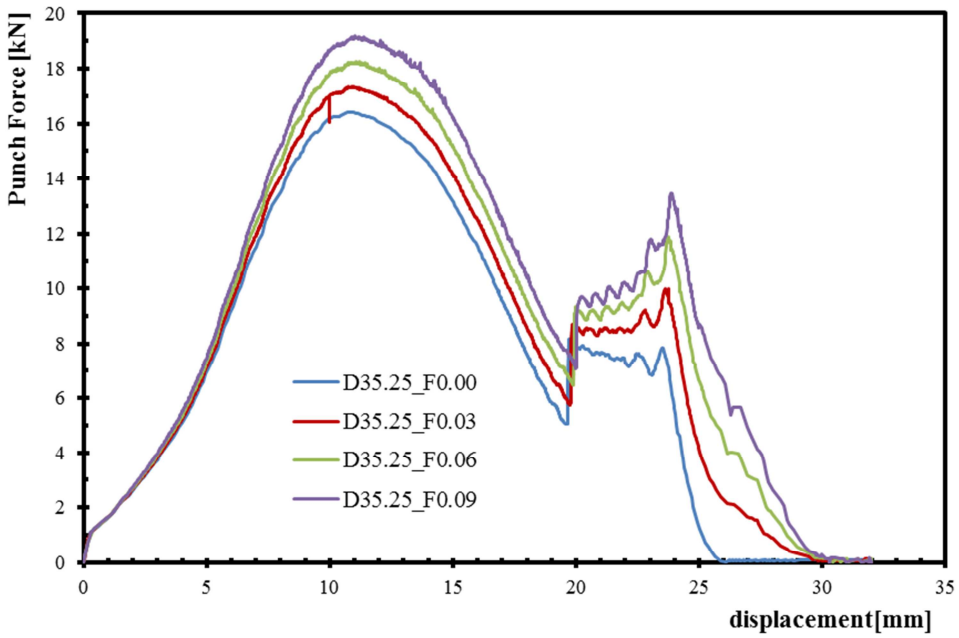

Figure 19 – Punch force evolution with the punch displacement in function of the global friction coefficient, for the model with anisotropic behaviour.

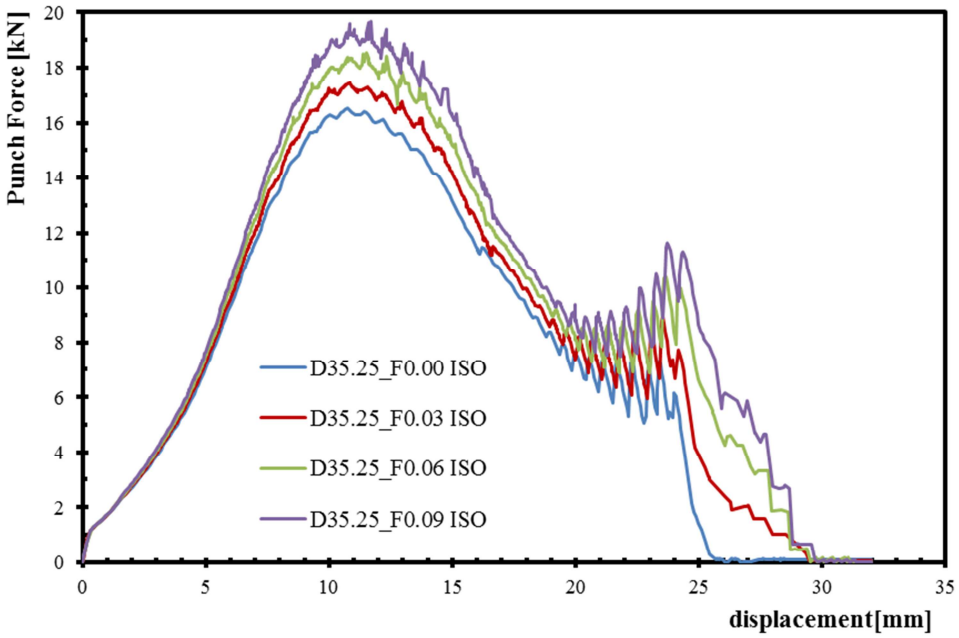

Figure 20 – Punch force evolution with the punch displacement in function of the global friction coefficient, to the model with isotropic behaviour.

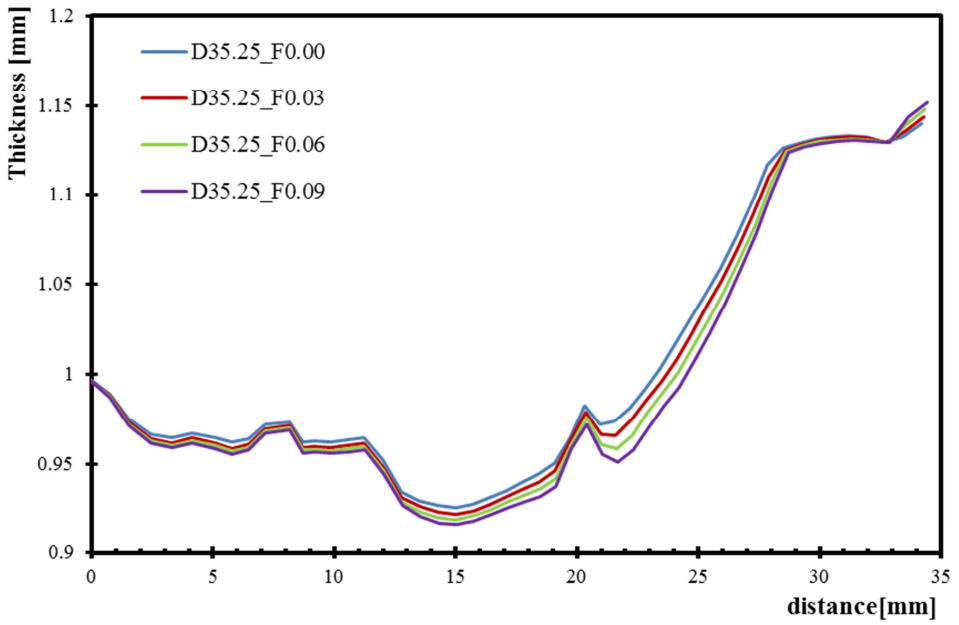

Figure 21 – Thickness evolution with the distance to blank's centre, along the RD, in function of the global friction coefficient, for the model with anisotropic behaviour.

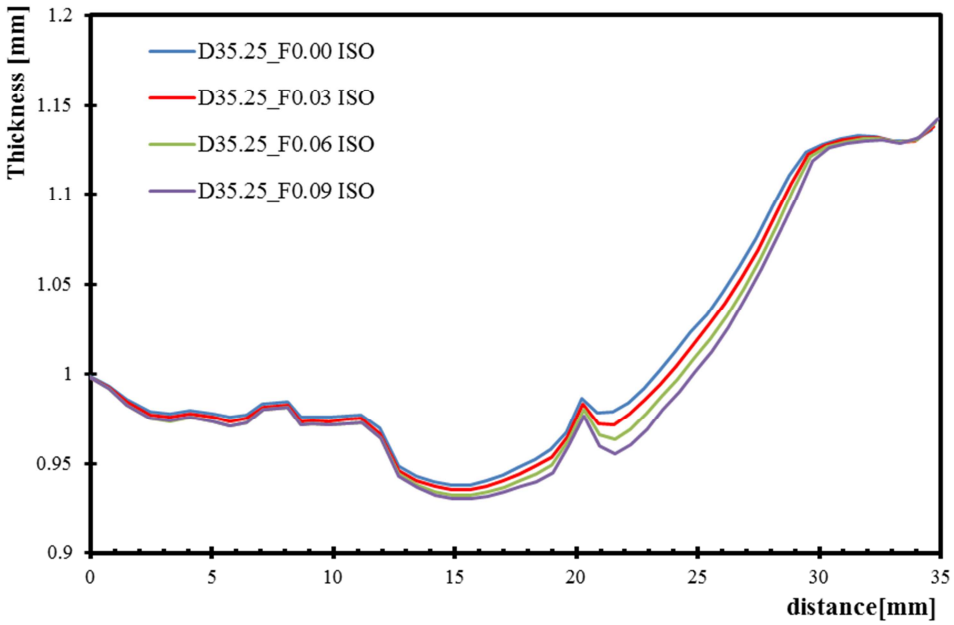

Figure 22 – Thickness evolution with the distance to blank's centre, along the RD, in function of the global friction coefficient, for the model with isotropic behaviour.

3.2.2. Tools friction coefficient

The friction is a parameter which depends of the contact between two surfaces. In deep drawing processes the friction depends of the contact between the tools and the sheet. The friction value represents the effect of the roughness surfaces', the tools material, the contact pressure, etc. In order to better understand the influence of the contact conditions between the sheet and each of the tools, in the deep drawing process, a simple set of tests was performed. These tests consisted in increasing the friction coefficient value of the surface under analysis, while keeping the values for the other contact surfaces constant. The idea is to increase the effect of the tool under study, compared with the effect of other tools, in order to better understand its influence on the process.

In the numerical simulations, a friction coefficient value of "0.09" was used has the highest value, while keeping the other contacting surfaces with a null friction coefficient value. For reference, a numerical simulation was performed considering a null global friction coefficient value. Note that for a friction coefficient value of "0.00", there is no friction force between the sheet and the tools in the process.

The numerical simulation results obtained for the punch force evolution during the deep drawing process are analysed in Figure 23. In the first stage of the curve, it is possible to confirm that the contact between the sheet and the blank-holder and the sheet and the punch has a negligible effect in the final result. In fact, only the contact between the sheet and the die seems to have an impact in the punch force evolution during the drawing process.

However, in the ironing stage it is necessary a more detailed analysis of the punch force evolution results. Due to the high contact pressures, this phase is more sensitive to the changes of all contact conditions, except the blank-holder. In fact, the blank-holder has no effect on the ironing process, since the sheet loses contact with this tool previously to the ironing process. During the ironing, the punch force evolution is only sensitive to the contact between the sheet and the die and the sheet and the punch. Comparing the results of the test D0P9BH0 with test D0P0BH0, after 25mm of punch advance, the difference in the punch force evolution clearly results from the effect of the contact between the sheet and the punch. The increase of the friction coefficient in the zone of contact between the sheet and the punch, reduces the material slip on the punch's wall. This results in a punch force increase and a decrease on the cup's height, which is also visible by comparing test D9P9BH9 with D9P0BH0. Figure 24 presents the cup's height evolution along the angle to the RD, for the different contact condition with each tool considered in this study. In this figure it is clearly observable the decrease of the cup's height when comparison test D9P9BH9 with D9P0BH0. The differences between test D0P9BH0 with test D0P0BH0 are not visible since they are inferior to 0.05 mm. However, they present an impact in the punch force evolution.

Figure 25 presents the thickness evolution with the distance to the cup's centre, at the end of the forming process. It is possible to confirm that the circular cup process is mainly dictated by the contact conditions between the die and the sheet (the thickness evolution is the same for D9P9BH9 and D9P0BH0).. Note that the curve of the test D0P9BH0 is overlap with test D0P0BH9.

Considering that in the experimental procedure all tools were made from the same material and manufactured using the same process, they should present the same roughness. In the numerical simulation the tools behave rigidly, therefore it is possible to consider that the influence of the tools is only due to the contact pressure. The contact

between the blank-holder and the sheet describes also the contact in the flange area, between the die and the sheet. Therefore, these contact regions should present similar contact pressure values. Then it is possible to consider that the friction in the process is mainly dependent of the contact conditions between the die inner radius and the sheet

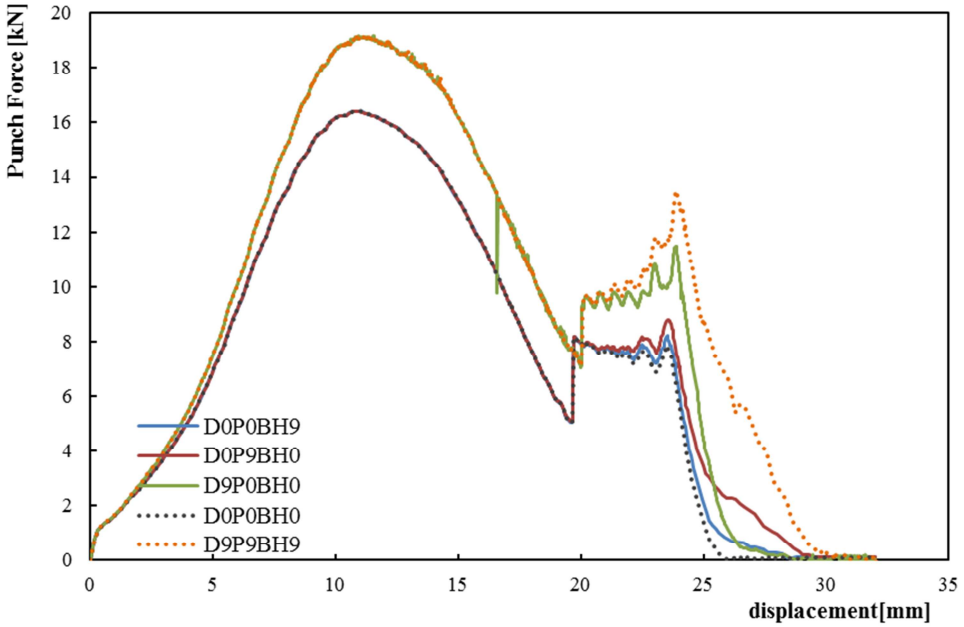

Figure 23 – Punch force evolution with the punch displacement, for the different contact condition with each tool.

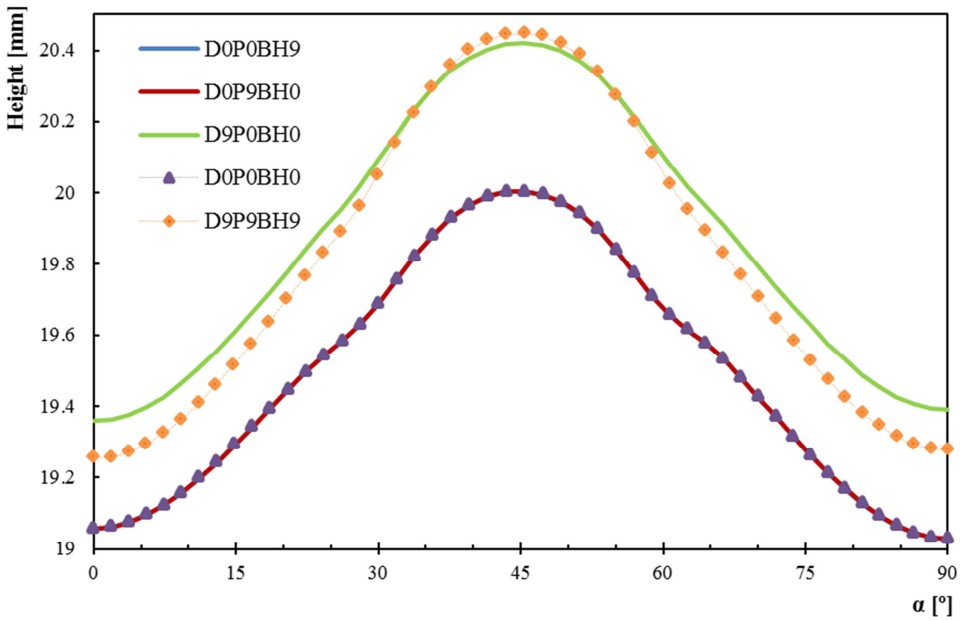

Figure 24 – Cup's height evolution along the angle to the RD, for the different contact condition with each tool.

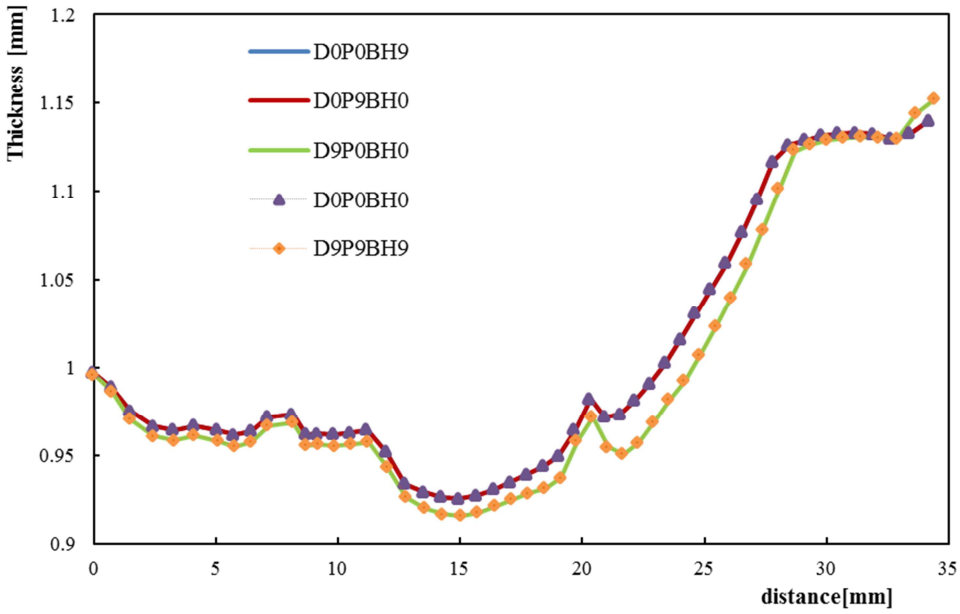

Figure 25 – Thickness evolution with the distance to blank's centre, along the RD, for the different contact condition with each tool.

Two forces are responsible for the ironing process, the normal/compression force and the tangential force. The normal forces represent the ones perpendicular to the cup's wall. The tangential forces correspond to the ones that appear due to the material flow into the die cavity. The shear on material results mainly from the tangential force. The

normal force is responsible for the strong compression of the material. For a null friction coefficient value there are no tangential forces acting on the blank sheet, only normal forces. On the opposite, the effect of the tangential force is higher for the global friction coefficient value of 0.09.

Figure 26 presents the normal force evolution with the punch displacement. These forces correspond to the radial force acting in the die, as predicted by the numerical simulation. It is observable the high increase of this force due to the ironing stage. When a global friction coefficient value of 0.09 is used the normal force attains the lower value, similar to the one obtained with a local friction value of 0.09 only in the die. Therefore, it seems that the decrease of the friction coefficient value causes an increase of the normal force, since it is necessary to impose a certain deformation to the material. The increase in the normal component of force justifies the decrease of the tangential component of the force, which leads to lower punch force values during the ironing process. In the numerical simulation the contact with friction is modelled using the Coulomb's law. Therefore, the tangential component of the force in the ironing zone is proportional to the contact force. Thus, the increase of the punch force during the ironing stage with the increase of the friction coefficient also results from the increase of the tangential forces. In fact, as shown in Figure 23, there is an important increase in the overall ironing punch force when a global friction coefficient value of 0.09 is used. In this analysis, it is also possible to identify two stage in the ironing stages. In the first stage the sheet is also being submitted to re-bending. The second stage corresponds only to ironing, and it starts for approximately 25 mm of punch displacement. For higher global friction coefficients values or higher values in the die radius, the starting of this second stage is delayed, because the draw-in is smaller for the same punch displacement.

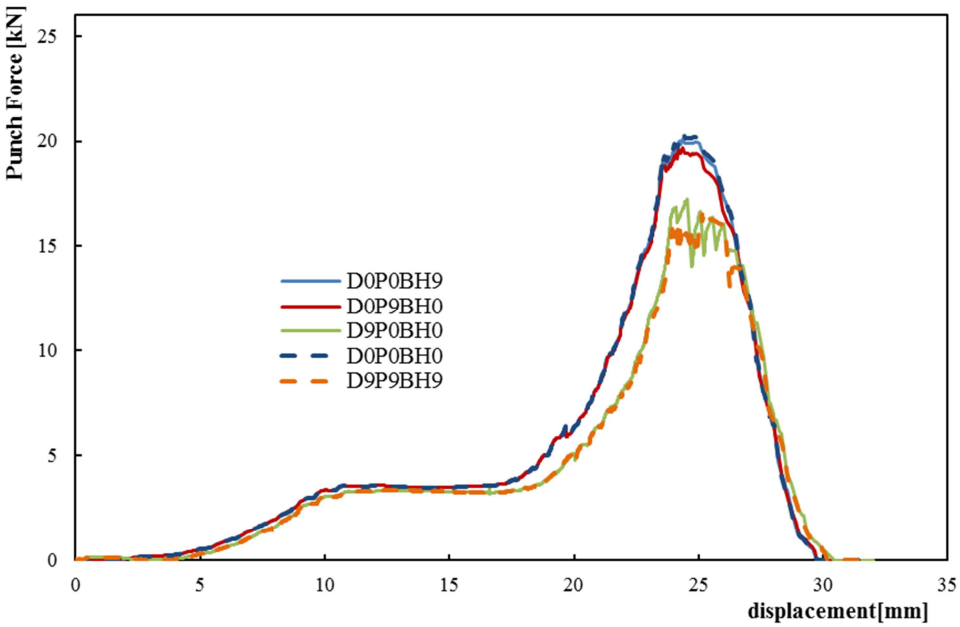

Figure 26 – Normal forces evolution with the punch displacement, for the different contact condition with each tool.

3.3. Maximum Punch force

Figure 27 presents the maximum values reported for the punch force evolution with the punch displacement, for each stage of the forming process. The green region represents the tests performed in the tools dimensions analysis. These results were all obtained with a constant global friction coefficient value of 0.06 and allow confirming the results previously presented in Figure 13 and Figure 14: the die opening diameter only affects the punch force during the ironing phase. The blue region represents the study of the friction conditions for the model with anisotropic material behaviour. As already shown in Figure 19 the punch force increases with the friction increase in both stages.. However, for the second stage it is also visible the effect of reduction the die opening diameter, which cause an increase in the punch force. The brown region represents the study of the friction conditions in the model considering the isotropic behaviour of the material. The results are similar to the ones obtained with the anisotropic model. However, there is an increase of the maximum punch force values for the drawing stage and a decrease for the ironing stage. The last region represents the effect of the contact

conditions between the sheet and the different tools. These results show that the die is the tool for which the contact conditions have the highest impact in the maximum punch force. However, in the ironing phase the punch also seems to have an effect, as previously explained.

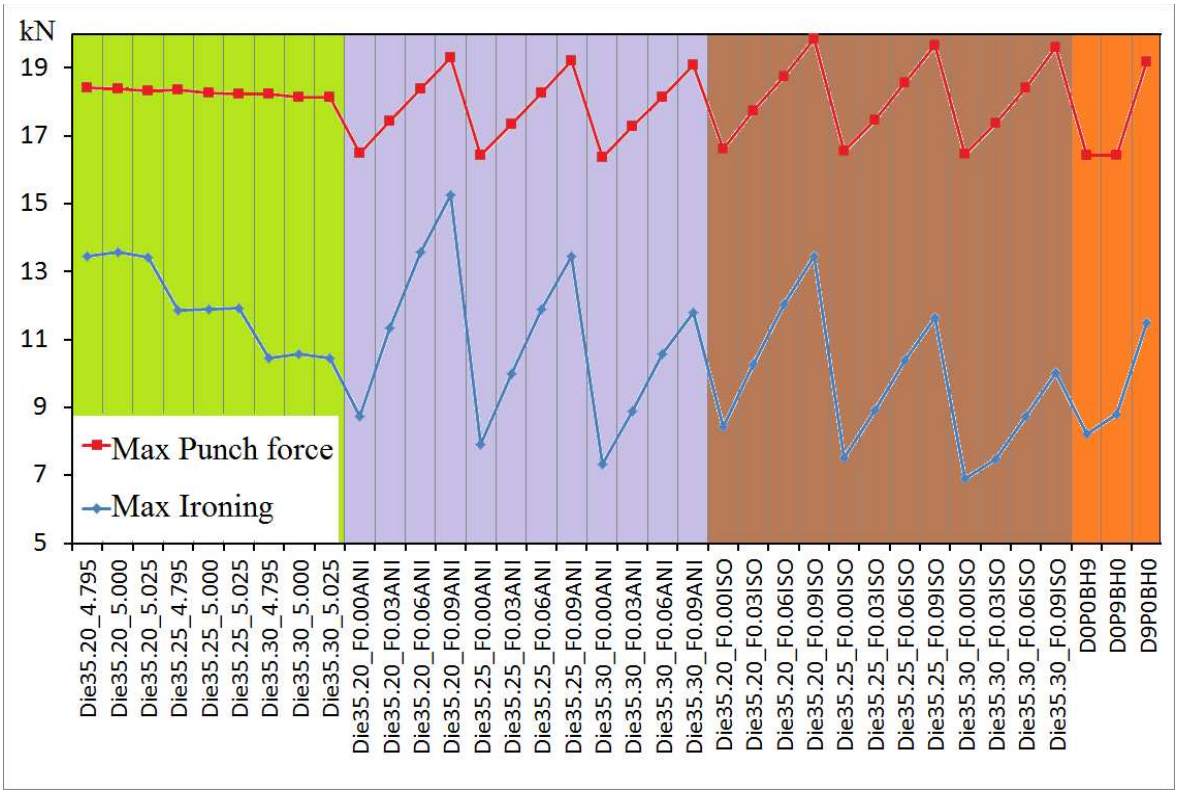

Figure 27 – Maximum values for the punch force numerically predicted for the drawing phase (Max) and the ironing stage (Max ironing).

3.4. Conclusions

In the die dimensions analyses it was observed that only the ironing phase is affected. The increase of force in this stage is due to the decrease of the "Die Opening Diameter", which causes a variation on the gap between the die and the punch. The increase of this gap results in an increase of the final cup's thickness and, consequently, in a decrease of the punch force. It was also observed that before the beginning of the ironing stage the variation of the "Die Opening Diameter" has a negligible effect on the final results.

In the global friction coefficient analyses the results show that the punch force increases with the increase of this parameter, both for the models considering isotropic or anisotropic material behaviour. Regarding the thickness evolution along the cup's wall, it was observed that in the re-bending and in the wall areas there is a thickness decrease associated with the increase of the global friction coefficient value.

Analysing the contact with friction conditions between the sheet and each tool, it was observed that the contact between the sheet and the die has the most important influence on the forming process. The contact conditions between the sheet and the blank-holder seem to have an negligible effect in the variables analysed, i.e. punch force evolution with its displacement and the thickness evolution along the cup's wall. The contact conditions between the sheet and the punch seem to have a small influence on the force evolution in the ironing phase.

4. EXPERIMENTAL ANALYSIS

Experimental analysis is often used in forming processes to test material properties and to validate numerical tests. The deep drawing of cylindrical cups is often used in numerical and experimental analysis, because it's a simple test that allows the comparison of different results. These cups are also used in Demeri's test to study the springback, as previously mentioned.

In chapter 1, a brief introduction about friction conditions influence in the deep drawing process was presented, as well as some details about the importance of the lubricant to help controlling these conditions. In this chapter, results of several experimental tests are presented, which were performed trying to understand the relation between the amount of lubricant and the friction coefficient. Thus, experimental tests were performed considering different amounts of lubricant. These tests also allowed an analysis of the different contact areas, previously presented in Figure 6. The lubrication regime during the deep drawing process is also studied, highlighting the anisotropy's importance in the lubrication regime of the flange area. Finally, the chapter ends with a comparison between numerical and experimental results.

Table 4 presents a resume of the experimental tests. Tests are divided in different colours for better understanding. Red represents tests without lubricant on both contact surfaces. In opposite, green represents tests with lubricant on both contact surfaces, excepting the contact between the punch and the sheet, since there is no movement between them and also based on the previous numerical results. Orange indicates the lubricant is used only to the contact surface between the blank-holder and the sheet. Blue indicates the lubricant is used only to the contact surface between the die and the sheet. All tests were done at room temperature and considering a constant drawing speed of 1m/s.

Table 4 – Experimental test.

Name	Lubricant on die-sheet (g/m^2)	Lubricant on b.h.-sheet (g/m^2)	Lubricant on punch-sheet (g/m^2)
Test3	0.0000	0.00	0.0000
Test12	8.3998	5.07	
Test13	20.2127	15.21	
Test14	45.7305	25.35	
Test17	0.0000	0.00	
Test18	0.0000	22.82	
Test19	20.1419	0.00	

4.1. Lubricant amount

Nowadays it's well known the lubricant's influence in friction coefficient reduction. Hence, it is possible to consider the variation of lubricant's quantity also changes the friction in the deep drawing process. Therefore, tests were performed considering three different amounts of lubricant, i.e. 8.4; 20.2 and 45.7 g/m^2 , according with the experimental procedure described in the section 2.2. The amount of lubricant was changed in blank's contact with the die and blank-holder's, leading to a sort of tests, summarized in Table 4.

The punch force evolution with its displacement, for the experimental tests performed with different amounts of lubricant in the blank, is presented in Figure 28. As it is observable, the lubricant's amount influence is negligible. Nevertheless, it is possible to note a small decrease of the maximum punch force in the drawing stage, with the increase of oil amount. The ironing phase is not influenced by the amount of oil used in the blank. The thickness evolution with the distance to the cup's centre is presented in Figure 29. As for the punch force evolution, the amount of lubricant presents a negligible effect in the thickness evolution along the cup's wall.

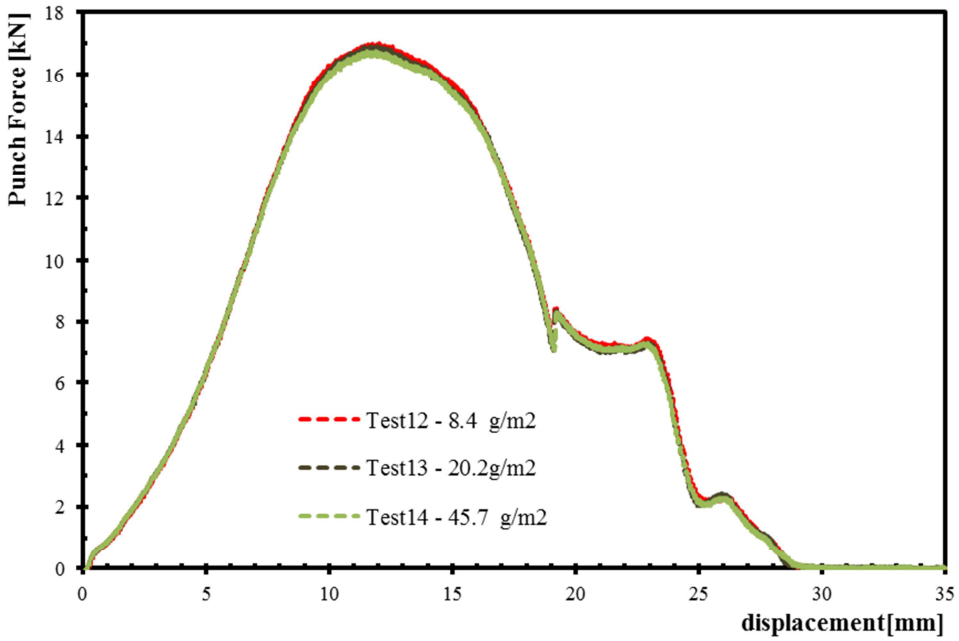

Figure 28 – Experimental punch force evolution with the punch displacement, for lubricant quantity of 8.4; 20.2 and 45.7 g/m^2 on the blank surface.

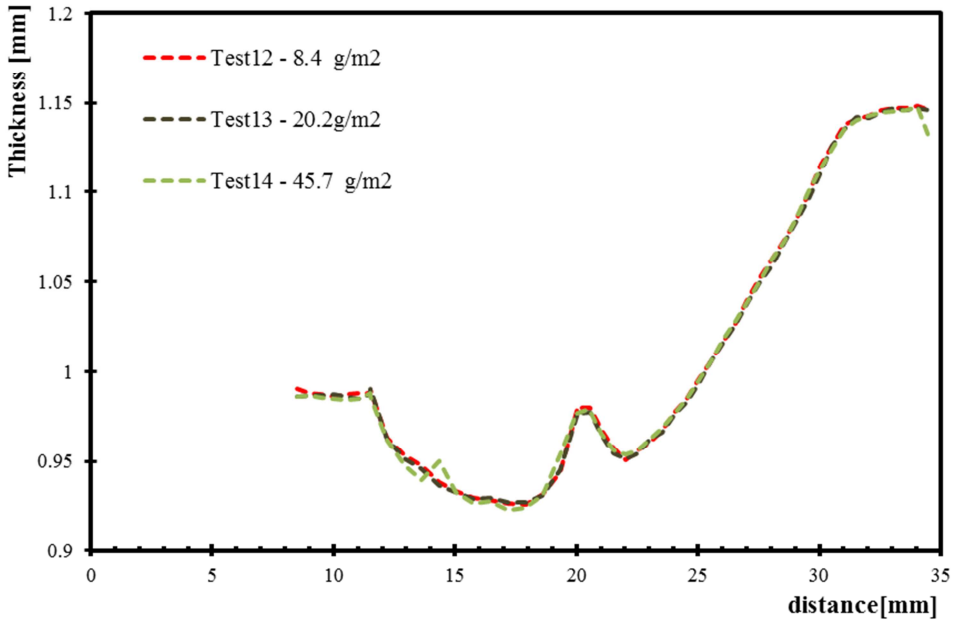

Figure 29 – Experimental thickness evolution with the distance to blank's centre, along the RD, for lubricant quantity of 8.4; 20.2 and 45.7 g/m^2 on the blank surface.

4.2. Lubrication conditions

To test the influence of contact conditions between each tool and the sheet, a simple test can be performed. This test consists in imposing a higher friction value to the tool surface in study, than the one of the other contacts surfaces. The idea is to increase the effect of the tool under study compared with the effect of the other tools, in order to better understand its influence on the process. Therefore, two tests were performed, one considering lubricant on the contact surface between the die and the sheet and another only with lubricant on the contact surface between the blank-holder and the sheet. Since there is no movement between the punch and the sheet and based on the previous numerical results, this study was not performed for the punch. These results are compared with the ones performed without lubricant and with those where there were lubricant in both tools.

Figure 30 presents the punch force evolution with the punch displacement. Comparing the evolution for test 19 with test 13, it is possible to observe that the amount of lubrication used on the blank-holder has a negligible effect on the punch force evolution. Figure 31 shows the thickness evolution along the cup's wall, measured from its centre. Although this figure seems to indicate that the thickness evolution of test 19 presents a higher thickness reduction on the re-bending and cup's wall area. It's also important to note an apparent difference in cup's bottom. Therefore, these results seem to confirm that the lubrication in contact surface between the blank-holder and the sheet does not have a relevant influence on this forming process.

The comparison of test 13 with test 18, for which no lubricant was applied on the contact surface between the die and the sheet, indicates that increasing of friction in this area leads to a high increase of the punch force, for both stages of the process. Nevertheless, the maximum values for the punch force are attained for the tests performed without lubricant, which can indicate some influence of the contact zones between the sheet and the blank-holder or the punch. Analysing the thickness evolution along the cup's wall, it is observable the overlap for the results of tests 19 and 18. Therefore, these results reveal a great importance of die and sheet's contact in forming forces and in thickness evolution. As expected, the lower thickness values are predicted for the test performed with lubricant.

Although, tests 3 and 17 were both performed without lubricant on the both tools, they present a clear difference on the punch force and thickness evolution. Test 3

presents higher punch force values and smaller thickness on the cup's wall, when compared with test 17. The only plausible reason for this difference seems to be the transfer of some finger grease to the tools surface and the sheet on test 17. In Figure 30 it is also visible a sudden increase of the punch force evolution for approximately 16 mm of punch displacement for both tests performed without lubricant. This can be related with the galling that occurs between the sheet and the die, for both tests.

Although the amount of lubricant seems to have a negligible effect in the process conditions, it is important to note that the use of lubricant, particularly in the contact surface between the die and the sheet, is fundamental to achieve a successful part. Also, it is possible to conclude that the use of lubricant reduces the punch force and increase the cup's thickness.

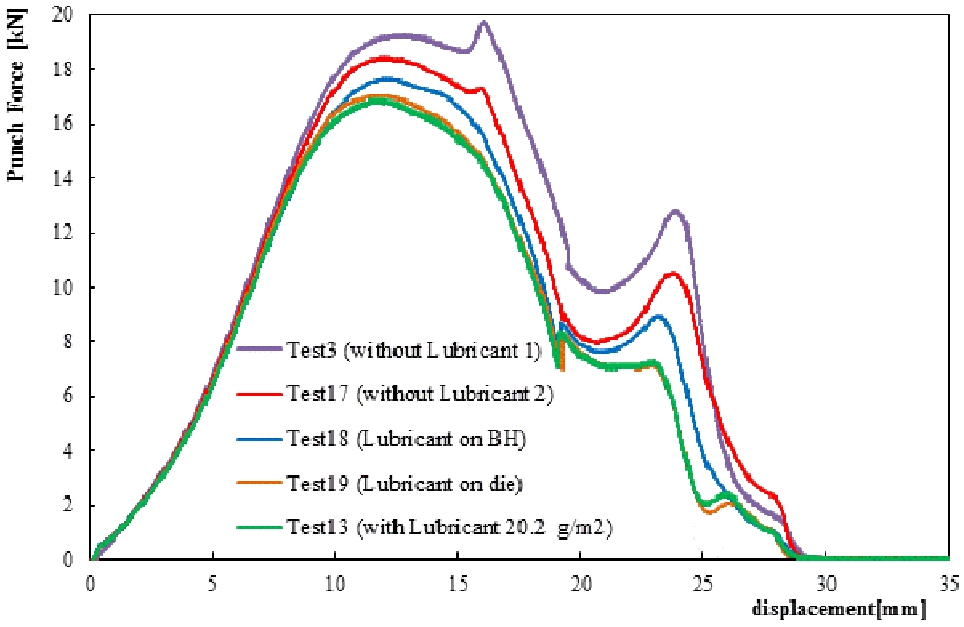

Figure 30 – Experimental punch force evolution with the punch displacement, for different contact conditions.

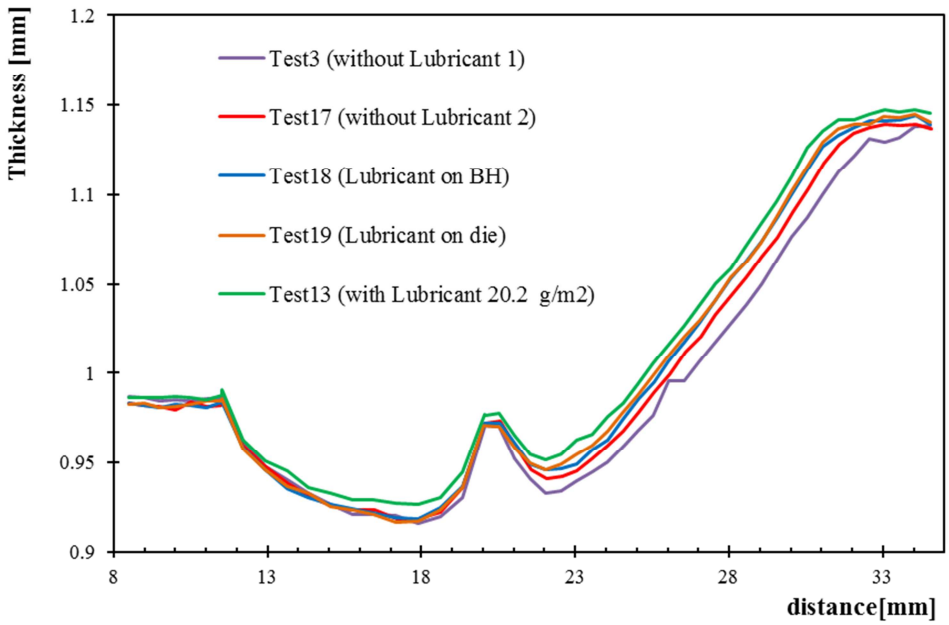

Figure 31 – Experimental thickness evolution with the distance to blank's centre, along the RD, for different contact conditions.

4.3. Contact pressure

As explained in second chapter, Schey (1983) describes six different contact regions in the deep drawing of a cylindrical cup. For each of these surfaces, a different contact pressure range can be associated. Figure 32 presents the cup geometry after a punch displacement of 12 mm, highlighting the lubricant distribution. It is possible to see that the different contact areas are linked with different lubrication regimes. In the contact areas 1 and 2, which represent the flange area, it is possible to observe only a few amount of lubricant. The contact area 3 (Die Inner Radius) seems to present no lubricant, there for a dry lubricant regime is present, similar the one present in region 4, 5 and 6. These differences on lubricant regime can be explained by the difference pressure on the contact areas.

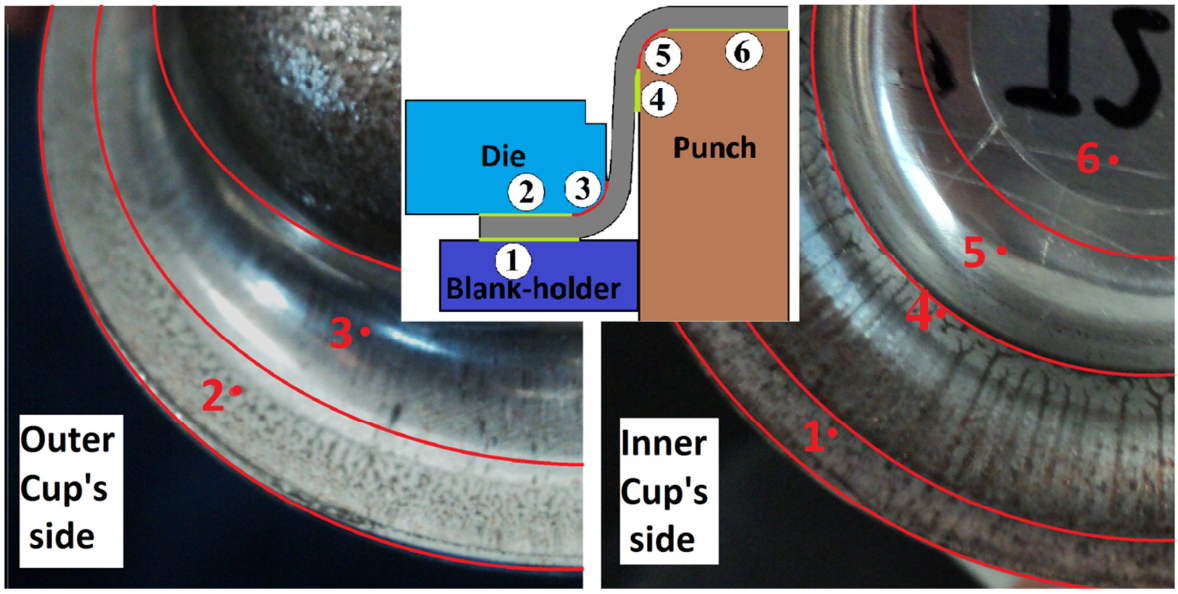

Figure 32 – Cup geometry after a punch displacement of 12 mm (1-contact sheet blank-holder; 2-contact sheet die in flange area; 3-contact sheet die radius's; 4-contact sheet punch flank; 5-contact sheet punch radius; 6-contact sheet punch bottom).

To better explain this assumption, a sheet with a high quantity of oil on its surface was compressed between the blank-holder and the die. Figure 33 presents the sheet surface before and after this compression phase. In Figure 33 a) the zones correspondent to contact with the blank-holder (area 1), with the die (area 2) and no contact (area 3) are identified previous to the compression test. Figure 33 c) presents the same areas after the test, highlighting the movement of the lubricant due to the holding force. In Figure 33 b) a schematic representation of the lubricant flow is presented It is possible to observe that, due the pressure of the flange area (area 1) the oil flows out from that area. Note that before the compression stage, the oil thickness is almost homogeneous, similar to the one obtained in sheet's region 3 after the test is performed. Some of the lubricant moves into the area that will be first in contact with the die inner radius (area 2), which can contribute to better lubrication conditions. Anyhow, some lubricant flows out from the contacting surfaces and it is lost. Thus, Figure 33 can help to confirm the results of Figure 28 and Figure 29, i.e. that the amount of oil on sheet surface is not so important because, even for a contact pressure of approximately 5.5 MPa, the lubricant flows out of the contact areas.

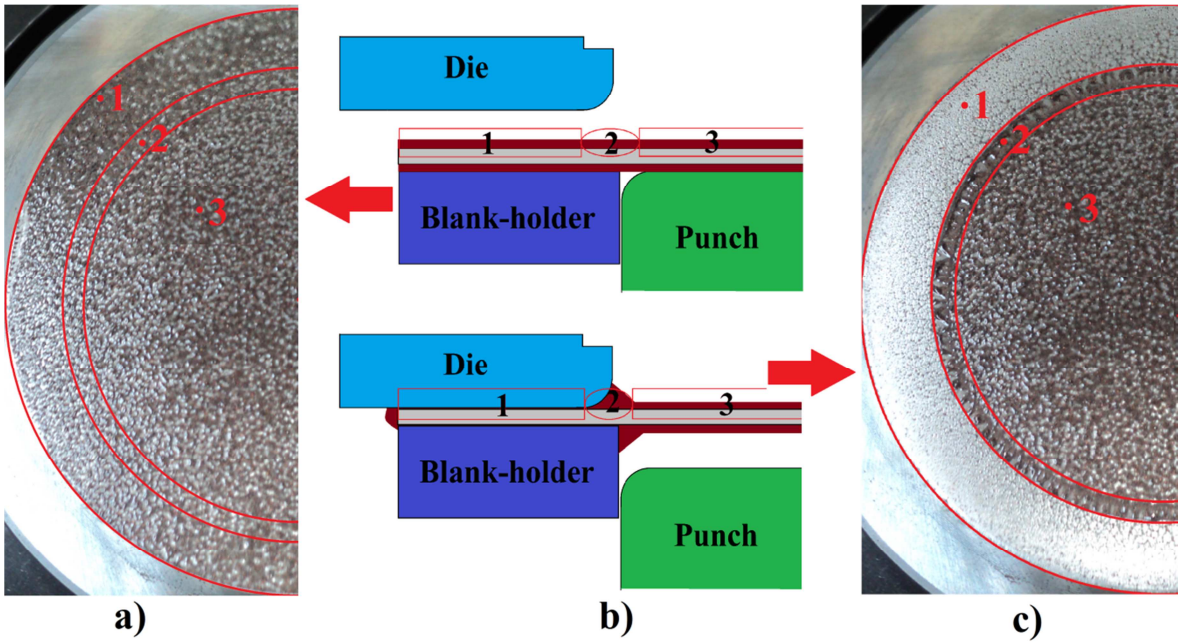

Figure 33 –a) Lubricant distribution on the sheet's surface before the compression between punch and die (Top view); b) Schematic representation of the lubricant flow; c) Lubricant distribution on the surface after compression between punch and die (Top view).

Figure 34 presents the result typically obtained for the punch force evolution with the punch displacement. In the figure are also presented the contact pressure distribution for the different steps of punch displacement. It is visible that the highest contact pressure values are always obtained in the Shey's region 3. Also the re-bending area (Shey's region 5) has an important contact pressure, but which is insignificant compared with pressure of region 3. These pressure results explain the lubricant distribution presented in Figure 32.

As opposed to punch force, the contact pressure is constantly increasing during the process, and during the ironing phase it attains its highest value. After this phase the pressure decreases until attaining the value of zero. The holding pressure at the beginning can be considered negligible compared with the global values attained during the process. Nevertheless, it is important to note that the holding pressure is increasing during the process due to the contact area decrease.

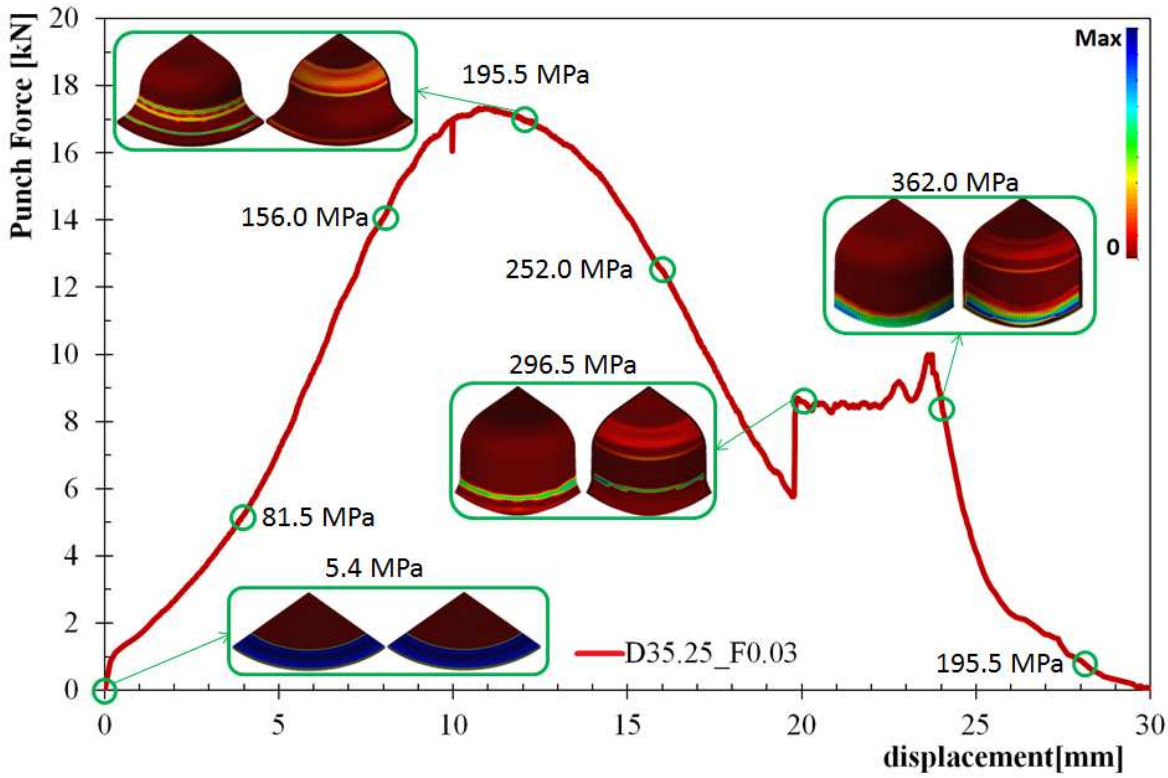

Figure 34 – Pressure distribution values for different punch displacement values, as well as maximum values for 0, 4, 8, 12, 16, 20, 24 and 28 mm of punch displacement.

4.4. Lubricant distribution

In the second chapter it was explained the influence of the contacting surfaces roughness in the sliding direction. During this study it was also observed that the anisotropy of the sheet also plays an important role in the lubrication regime. The non-homogeneous deformation of the material with the angle to the RD has an important effect in the pressure distribution on flange area. Figure 35 presents the geometry of a cylindrical cup, corresponding to a punch displacement of 16 mm, which corresponds to the displacement just before the loss of contact between the sheet and the blank-holder. Region 1 corresponds to the die's flange area and region 2 is the deep drawn cup. The green points presented in the die's flange area highlight pools of lubricant that remain in the die surface. Note that this amount of lubricant is present for 45º, 135º, 225º and 315º to RD, which correspond to the directions with higher thickness reduction due to the anisotropic behaviour of the material.

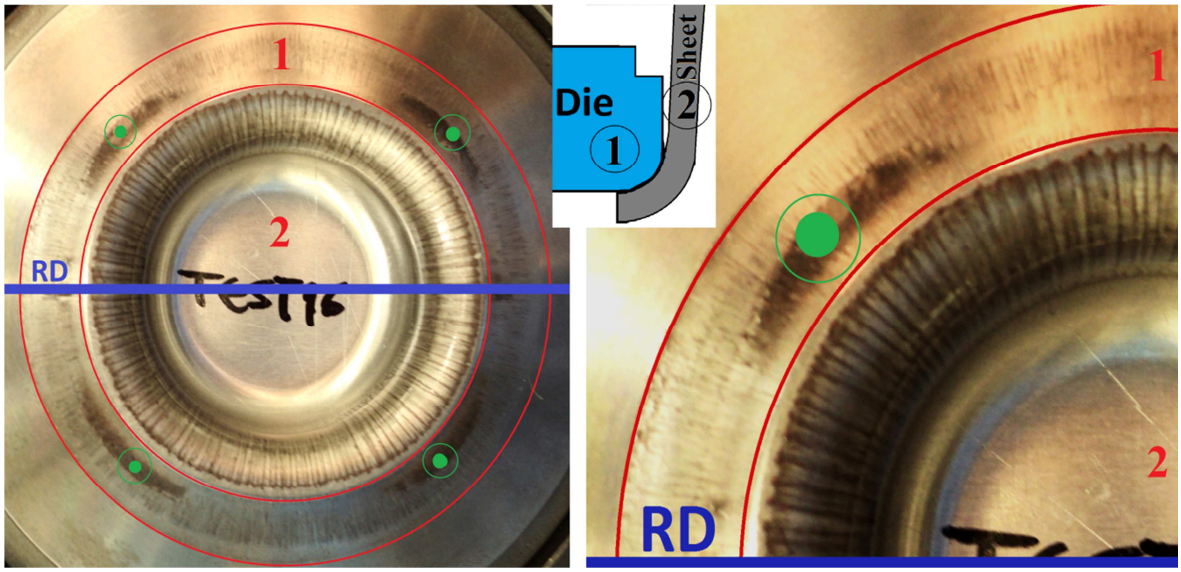

Figure 35 – Cup geometry after a punch displacement of 16mm. The green points represent pools of lubricant on die surface's to 45º, 135º, 225º and 315º to RD. → 1 – Flange are of die; 2 – Cup.

Figure 36 presents an analysis of the thickness evolution with the angle to RD, in the outer surface of the flange area. These are numerical results obtained for punch displacements of 4, 8, 12, 16, 20 and 24 mm. It is possible to observe the thickness reduction for the orientation corresponding to 45º to the RD. This thickness reduction in flange area creates the free space for the lubricant flow. Due to the higher contact pressure close to the RD and TD, the lubricant flows from there directions into the free space in the regions near 45º to RD, creating the pools. By this reason, it is possible to consider that the contact on flange for the direction corresponding to 0º, 90º, 180º and 270º is almost dry.

Figure 37 shows the lubricant distribution in the blank-holder, after 16 mm of punch displacement. At this stage the oil distribution on blank-holder surface seems to be homogeneous. Thus, it is possible to consider that the pressure in the contact surface between the sheet and the blank-holder is almost homogeneous, i.e. that the material's anisotropic effect has no influence on the lubricant regime in this surface. Therefore, this result indicates that the thickness variation with the angle to the RD only affects the contact surface between the sheet and the die.

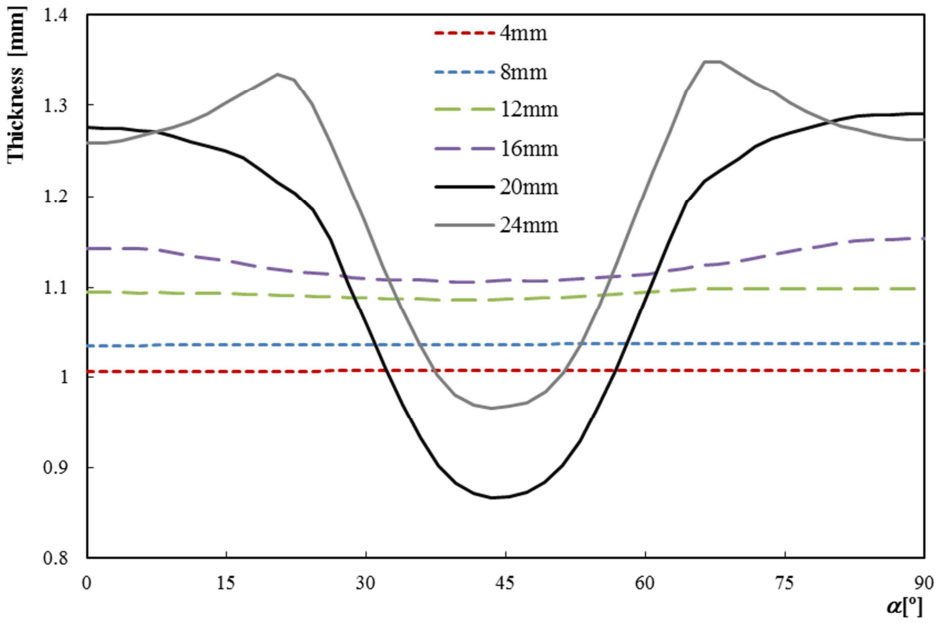

Figure 36 – Thickness evolution with the angle to RD along the flange outer surface, for 4, 8, 12, 16, 20, 24 mm of punch displacement.

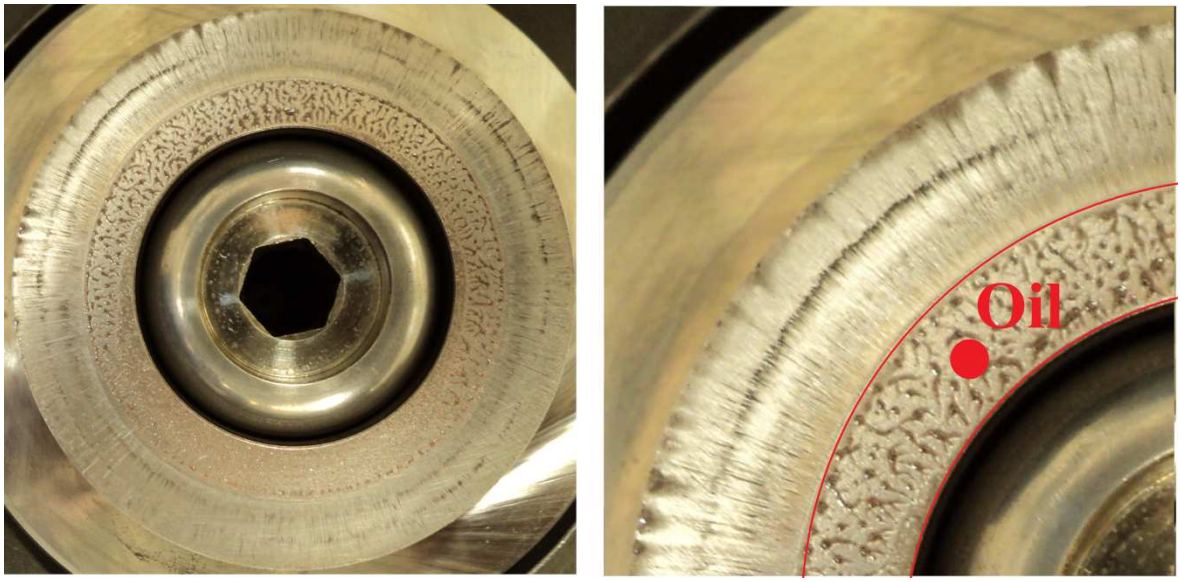

Figure 37 – Blank-holder surface's after 16mm of punch displacement. Blank-holder surface's presents an homogeneous distribution of lubricant in the sheet area (flange), as shown in the detail presented in the right.

4.5. Numerical vs. Experimental

The comparison between numerical and experimental results is performed in this section. The numerical results correspond to the die with an opening radius equal to 35.25, a constant friction coefficient value of 0.03, considering isotropic (D35.25_F0.03ISO) and anisotropic (D35.25_F0.03ANI) material mechanical behaviour. The experimental results correspond to Test 13, for which both contact zones were lubricated. Figure 38 presents the comparison of the punch force evolution with its displacement. Figure 39 compares the thickness evolution along the cup's wall, along the RD.

In this Figure 39 it is observable that in the ironed zone, the experimental test, presents a thickness value higher than the numerical model. It is important to mention that the thickness calculated for the numerical results is not accurate when shear occurs. That is why the numerical results present a small increase in the cup's top. The thickness' difference in the ironed zone can only results from a higher gap between the punch and the die in the experimental tools than in the ones used in the numerical model. The results of Figure 13 show that an increase on the gap between the punch and the die leads to a decrease of the punch force during the ironing phase. Thus, this difference can also help to explain why the maximum force in the ironing phase predicted by the numerical results is globally higher (see Figure 38).

The global friction value of 0.03 was selected for the numerical simulation results based on the maximum punch force during the drawing stage. However, it is important to mention that this is not the global friction value that leads to a better comparison in terms of thickness evolution. In fact, numerical simulations performed with a global friction coefficient value of 0.09 present a thickness evolution closer to the experimental one. Nevertheless, as showed during this study, the friction coefficient value is different in each contact area. Therefore, it is difficult to establish a global friction coefficient value able to accurately capture all the process conditions.

Analysing Figure 38 and Figure 39 the model that considers an isotropic behaviour of the material seems to lead to a better approximation to the experimental ones. In fact, the Hill'48 yield criterion, used in the anisotropic behaviour model, is known for not representation accurately this type of materials (r<1). However, in order to accurately identify more appropriate yield criteria it is important to have more experimental data

available, in order to better describe the biaxial strain path. Therefore, taking into account the results available it was considered a good option. In fact, the Hill´48 yield criterion can give particularly inaccurate results for the biaxial strain path. Although, this path is not predominant in this forming process, the cup bottom follows strain paths close to it. This can explain why the von Mises yield criteria leads to better prediction of the thickness evolution in the cup's bottom. The objective of this work was not to make a direct comparison between the numerical and the experimental results, but to understand better the influence of some process variables. In fact, the work presented here highlights that many factors can lead to important differences between the experimental test and the numerical model.

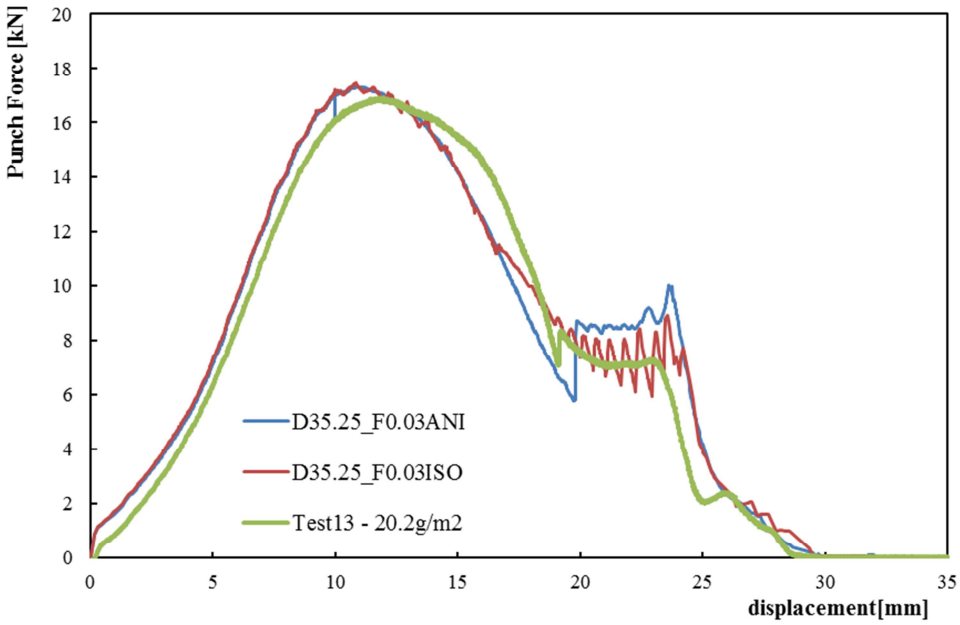

Figure 38 – Punch force evolution with the punch displacement, analysing isotropic case, anisotropic case and experimental test 13.

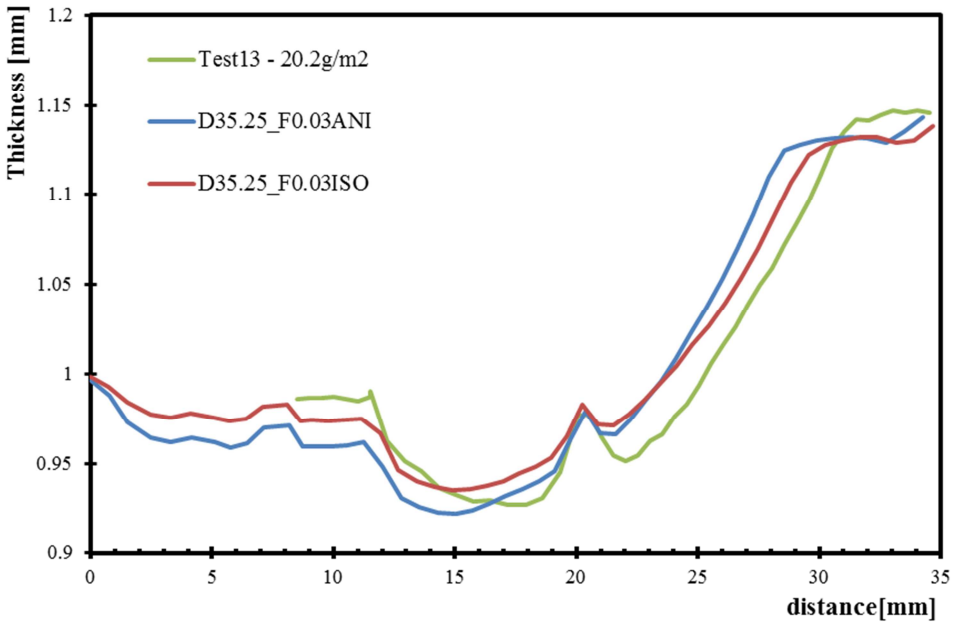

Figure 39 – Thickness evolution with the distance to blank's centre, along the RD, analysing isotropic case, anisotropic case and experimental test 13.

4.6. Conclusions

The results of the experimental tests show that the influence of the amount of lubricant is negligible in the punch force and thickness evolution. Nevertheless, it is possible to note a small decrease of the punch force with the increase of the amount of oil on the drawing stage. Regarding the lubricant conditions on the different tools, the experimental results are very sensitive to this factor. When no lubricant is applied in the contact surface between the die and the sheet, there is a high increase in the punch force evolution and a high thickness decrease of the cup's wall. In fact, both test without lubricant resulted in galling of the sheet surface. However, this process variable is not affected by the contact conditions between the sheet and the blank-holder. Regarding the thickness evolution along the cup's wall, it is affected by both contact conditions in the die and with the blank-holder. Concluding, the lubricant have an effect to reduce the forces and to avoid the galling thickness reduction, but its amount is not so important.

The experimental tests also show that the different contact areas described by Schey (1983) are correlated with different lubrication regimes, and that there is lubricant

flow from zones with higher contact pressure to ones with lower. This effect leads to pools of lubricant located at 45º to the RD, due of the anisotropic behaviour of the material. The comparison between numerical simulation and experimental results also helps in the interpretation of the process conditions. However, the numerical model still needs to be improve in order to better describe the experimental test. In particular, it is important to improve the description of the material mechanical behaviour.

5. CONCLUDING REMARKS

This work focused in the study of the deep drawing of a cylindrical cup, using an AA5754-O blank. The study involved both a numerical and experimental analysis of the forming process. The process conditions defined for the experimental tests, performed in a Zwick/Roell-BUP200 machine, include a constant blank-holder force of 6kN, room temperature, and a constant drawing speed of 1mm/s. The numerical simulations were performed with the in-house code DD3IMP.

The numerical study performed involved a parametric analysis of the influence of the die's dimensions (diameter and shoulder radius) and the global and local friction coefficient, between the sheet and each tool. Regarding the die's dimensions, it was observed that the variation of the "Die Opening Diameter" was the only parameter affecting the forming process, particularly the ironing stage. This influence results from the variation it induces on the gap between the die and the punch. The increase of this gap leads to an increase on the final cup's thickness and a decrease of the maximum punch force, in the ironing stage.

Regarding the global friction coefficient, its increase leads to the higher punch force values and to a decrease of thickness along the cup's wall. These results were predicted by the numerical model and confirmed in the experimental tests. Note that the friction increase corresponds to a decrease of the amount of lubricant. The experimental results indicate that the amount of lubricant has a negligible effect in the final results, i.e. in the punch force and thickness evolution. Although the amount of lubricant seems to be negligible, when no lubricant is applied in the contact surfaces galling occurs. These results indicate that maybe lower amounts of lubricant should be tested in order to better understand the effect of this variable.

The analysis of the contribution of each contact zone between the sheet and the tools in the process, using both the numerical model and experimental tests, lead to similar results. The contact between the sheet and the die has the highest influence in the process. In fact, according to the numerical results this is the zone were the higher pressure values occur. Therefore, this can result in higher friction coefficient values in the experimental tests. The experimental analysis also enabled to verify the effect of the pressure in the

different contact region, described by Shey (1983), concerning the lubricant distribution. This distribution is also affected by the material mechanical properties. In this particular case, the lower increase of the sheet thickness along the 45º to the RD, allows the forming of pools of lubricant.

Globally, the analysis performed based on numerical and experimental results lead to the same final conclusions. However, the direct comparison of these results highlight some differences, which indicate that the numerical model still needs to be improves, in particular the mechanical characterization of the material's mechanical behaviour.

REFERENCES

[Coër 2009] – J. Coër (2009), "Comportement élasto-plastique d'une tôle métallique à haute température", Rapport de stage de Université de Bretagne-Sud.

[Coër et al 2010] – J. Coër, C. Bernard, H. Laurent, A. Andrade-Campos, S. Thuillier (2010), "The effect of temperature on anisotropy properties of an aluminium alloy", Experimental Mechanics, 51, 1185-1195.

[Coles et al 2010] – Jeffrey M. Coles, Debby P. Chang, Stefan Zauscher, (2010), "Molecular mechanisms of aqueous boundary lubrication by mucinous glycoproteins", Current Opinion in Colloid & Interface Science, 15, 406–416. http://www.sciencedirect.com/science/article/pii/S1359029410000786

[Demeri et all 2000] – Demeri, M.Y., Lou M., Saran, M.J., "A benchmark test for springback simulation in sheet metal forming", Society of Automotive Engineers, Inc., vol. 01-2657.

[Figueiredo et al 2011] – L. Figueiredo, A. Ramalho, M. C. Oliveira, L. F. Menezes (2011), "Experimental study of friction in sheet metal forming", Wear, 271, 1651-1657.

[Emmens, 1997] – Emmens,W.C.(1997). "Tribology of flat contacts and its application in deep drawing", PhD thesis, University Of Twente, ISBN: 90-3651028-7.

[globalspec] – http://www.globalspec.com/reference/63587/203279/chapter-9-drawn-parts

[Grèze, 2009] – R. Grèze (2009), "Experimental and numerical study of springback of aluminium alloys after drawing", PhD thesis, University Of Bretagne-sud.

[Guillon et al 2001] – O. Guillon, X. Roizard, P. Belliard (2001), "Experimental methodology to study tribological aspects of deep drawing – application to aluminium alloy sheets and tool coatings", Tribology International, 34, 757–766.

[Halim et al 2007] – Herdawandi Halim, David S. Wilkinson, Marek Niewczas, (2007) "The Portevin–Le Chatelier (PLC) effect and shear band formation" Acta Materialia, 55, 4151–4160. http://mse.eng.mcmaster.ca/faculty/niewczas/PDF

files/The PortevinLeChatelier (PLC) effect and shear band formation in AA5754 alloy.pdf

[Han, 1997] – S.S.Han (1997), "The influence of tool geometry on friction behavior in sheet metal forming", Journal Of Materials Processing Technology, 63, 129-133.

[Hsu et al, 2002] – Hsu, C. W., Ulsoy, A. G., et Demeri, M. Y., (2002), "Development of process control in sheet metal forming", Journal of Materials Processing Technology, 127, 361-368.

[Laurent et al 2008] – H. Laurent, R. Grèze, P. Y. Manach, S. Thuillier (2008), "Influence of constitutive model in springback prediction using the split-ring test", International Journal of Mechanical Sciences, 51, 233 – 245.

[Laurent et al 2010] – H. Laurent, R. Grèze, M. C. Oliveira, L. F. Menezes, P. Y. Manach, J. L. Alves (2010) "Numerical study of springback using the split-ring test for an AA5754 aluminum alloy", Finite Elements in Analysis and Design, 46, 751-759.

[Laurent et al 2011] – H. Laurent, J. Coër, R. Grèze, P. Y. Manach, A. Andrade-Campos, M. C. Oliveira, L. F. Menezes (2011), "Mechanical behaviour and springback study of an aluminium alloy in warm forming conditions", ISRN Mechanical Engineering, 2011, Article ID 381615.

[Magny, 2002] – C. Magny (2002), "Friction laws dedicated to the numerical simulation of deep drawing" Revue de Métallurgie, 99, 145-156

[Oliveira et al 2011] – M. C. Oliveira, L. F. Menezes, H. Laurent, J. Coër, P. Y. Manach, J. L. Alves (2011), "Numerical simulation of the deep drawing of a cylindrical cup with ironing", Tadeu, A Figueiredo, I.N.; Menezes, L.F.; Mendes, P.A.; Rodríguez-Ferran, A.; Arias, I.; Blanco, J.M., Congress on Numerical Methods in Engineering 2011, Portugal, 14 to 17 June, 440-443.

[Özek and Bal, 2009] – Cebeli Özek, Muhammet Bal (2009), "The effect of die/blank holder and punch radiuses on limit drawing ratio in angular deep-drawing dies", Int J Adv Manuf Technol, 40, 1077–1083.

[Park and Niewczas, 2008] – Dong-Yeob Park, Marek Niewczas (2008), "Plastic deformation of Al and AA5754 between 4.2K and 295K", Materials Science and Engineering, A 491, 88–102.

[Roizard et al 1999] – X. Roizard, F. Raharijaona, J. von Stebut, P. Belliard (1999), "Influence of sliding direction and sliding speed on the micro-hydrodynamic lubrication component of aluminium mill-finish sheets", Tribology International, 32, 739–747.

[Schey, 1983] – Schey, J.A.(1983). "Tribology in metalworking – friction, lubrication and wear", ISBN-13: 978-0871701558

[Westeneng, 2001] – André Westeneng (2001), "Modelling of contact and friction in deep drawing processes", Phd Thesis, University of Twente, ISBN:90-365-1549-1c

[Xia et al, 2004] – Xia, C., Miller, C., et Ren, F. (2004), " Springback behavior of aa6111-t4 with split-ring test" Materials Processing and Design, 712, 934-939.

[Wikipedia, (2012)a] – http://en.wikipedia.org/wiki/Deep_drawing

[Wikipedia, (2012)b] – http://en.wikipedia.org/wiki/Portevin%E2%80%93Le_Chatelier_effect

ANNEX A

FICHE PRODUIT ET D'INFORMATIONS TECHNIQUES

GRAISSE HAUTES TEMPERATURES

Industrie

Réf :5411.doc

1. CARACTERISTIQUES PRINCIPALES

La GRAISSE HAUTES TEMPERATURES est un lubrifiant micro-métal de haute performance pour les cas extrêmes ; elle permet d'assurer une lubrification d'assemblages entre -40°C à +1200°C. Insensible à l'eau et à la corrosion, cette graisse sans silicone apporte en outre des propriétés d'étanchéité, d'anti-corrosion, et est anti-grippante.

2. DOMAINE D'APPLICATION

La GRAISSE HAUTES TEMPERATURES trouve son application dans les domaines suivants :

- Joints et clapets de chaudières, brûleurs, régulateurs, convoyeurs,
- Pièces automobiles, cosses de batterie, chaînes, câbles, mécanismes de grues,
- Industrie chimique, matériels agricoles, travaux publics...

3. UTILISATION - MODE D'EMPLOI

Bien agiter l'aérosol de manière à décoller la bille. Éliminer les anciennes graisses, vaporiser par pressions courtes sur les assemblages à protéger. Faire pénétrer la graisse en manœuvrant les pièces lubrifiées. Après pulvérisation, purger l'aérosol la tête en bas pour éviter un bouchage par les particules métalliques.

4. CARACTERISTIQUES PHYSICO-CHIMIQUES

Produit actif :

- Aspect :	liquide épais de couleur métallique		
- Fluide de base :	huile minérale	- Viscosité de l'huile :	95 cSt à 40°C
- Masse volumique à 20°C :	0.80 g/cm^3	- Tenue en température :	-40°C à +1200°C
- Épaississant :	inorganique	- Point de goutte :	sans
- Pénétrabilité :	310 - 340 (NLGI 1)	- Point d'écoulement :	-9°C
- Teneur en lubrifiants solides :	16%	- Résistance à la pression dynamique : 10 tonnes/cm^2	
- Coefficient de friction :	inférieur de 30% aux huiles ou graphite		
- Protection en chaleur humide :	5000 heures à 50°C - 100% H.R.		

- Inflammable
- Ne contient pas de silicone

5. PRECAUTIONS D'EMPLOI

Consulter la fiche de données de sécurité.

Récipient sous pression.

Ne pas fumer. Ne pas vaporiser vers une flamme ou un corps incandescent. Ne pas jeter au feu même vide. Conserver hors de portée des enfants. Ne pas respirer les aérosols. Bien ventiler après usage.

6. CONDITIONNEMENT ET STOCKAGE

Aérosol de 520 ml (12 aérosols / carton). Référence 5411.

A protéger contre les rayons solaires et à ne pas exposer à une température supérieure à 50°C. Ne pas percer ou brûler même après usage. Conserver à l'écart de toute flamme ou source d'étincelles ou d'ignition.

Conserver à l'abri de l'humidité et sous abri, dans un endroit bien ventilé et aéré.

Cette fiche technique a été établie le 12/07/99 et annule toutes les fiches précédentes. Les renseignements fournis sont basés sur nos connaissances et notre expérience à ce jour. Ils ne peuvent en aucun cas impliquer une garantie de notre part ni engager notre responsabilité quant à l'utilisation de nos produits.

ITW Produits Chimiques 112, bd de Verdun – BP 306 92402 Courbevoie cedex FRANCE ☎ : 01 41 88 89 00 1/ 1